# Grid Integration of AI Data Centers: A Critical Review of Energy Storage Solutions

Sina Mohammadi, Wayne Wang, Marcus Chen I Wada, Rouzbeh Haghighi, Ali Hassan, Hualong Liu, Archit Bhatnagar, Ang Chen, Wencong Su

***Abstract*—Artificial intelligence (AI) is driving a rapid expansion of data centers (DCs). These facilities consume large amounts of electricity and introduce new challenges for power systems. AI workloads cause rapid power changes and high peak demand. These behaviors are different from traditional data centers (TDCs) and can affect grid stability and reliability. This paper reviews how energy storage systems (ESSs) can help integrate AI data DCs with the electric grid. We examine storage solutions at multiple levels, including grid-scale batteries, UPS systems, rack-level storage, and chip-level buffering. Each layer operates at a different time scale and serves a different purpose. Grid-interactive UPS (GiUPS) systems can respond quickly to disturbances and assist with frequency regulation or voltage ride through. Large battery energy storage systems (BESSs) can smooth power demand, support renewable on-site generation, and provide grid services. Rack-level and server-level storage help manage fast power fluctuations close to computing hardware. We also discuss other technologies such as fuel cells (FCs) and thermal energy storage (TE) that can support co-generation and reduce emissions. In addition, second-life battery energy storage (SLBESS) are reviewed as a lower-cost option for large installations whether supporting UPS battery or as a backup generation. The paper compares the benefits, challenges, and coordination requirements of these solutions. Overall, the study provides a structured view of how energy storage can improve reliability, flexibility, and sustainability when connecting future AI data centers to the power grid.**

***Index Terms*—AI data center, battery backup unit (BBU), battery energy storage systems (BESS), fuel cell (FC), GPU, second-life battery energy storage systems (SLBESS), thermal energy storage (TES), UPS**

## ABBREVIATIONS

| | |
|---|---|
| AI | Artificial Intelligence |
| AWS | Amazon Web Services |
| BBU | Battery Backup Unit |
| BESS | Battery Energy Storage System |
| BMS | Battery Management System |
| BTM | Behind-the-Meter |
| CapEx | Capital expenditures |
| CPU | Central Processing Unit |
| DC | Data Center |
| DMA | Direct Memory Access |
| DoD | Depth of Discharge |
| DVFS | Dynamic Voltage and Frequency Scaling |
| EMS | Energy Management System |
| ESS | Energy Storage System |
| EV | Electric Vehicle |
| FC | Fuel Cell |
| FFR | Fast Frequency Response |
| FTM | Front-the-Meter |
| GFL | Grid-Following |
| GFM | Grid-Forming |
| GiUPS | Grid-interactive Uninterruptible Power Supply |
| GPU | Graphics Processing Unit |
| HBM | High Bandwidth Memory |
| HDD | Hard Disk Drive |
| HPC | High Performance Computing |
| HVRT | High Voltage Ride Through |
| IEC | International Electrotechnical Commission |
| LFP | Lithium Iron Phosphate |
| LLM | Large Language Model |
| LV | Low Voltage |
| LDESSs | Long Duration Energy Storage Systems |
| LVRT | Low Voltage Ride Through |
| MV | Medium Voltage |
| MVDC | Medium Voltage Direct Current |
| OCP | Open Compute Project |
| ORV3 | Open Rack V3 |
| PCC | Point of Common Coupling |
| PDU | Power Distribution Unit |
| PEMFCs | Polymer Electrolyte Membrane Fuel Cells |
| PLL | Phase Locked Loop |
| PPA | Power Purchase Agreement |
| PSA | Power Sharing Unit |
| RDMA | Remote Direct Memory Access |
| RES | Renewable Energy Sources |
| SLB | Second Life Battery |
| SLBESS | Second-Life Energy Storage System |
| SoC | State of Charge |
| SOFCs | Solid Oxide Fuel Cells |
| SoH | State of Health |
| SSD | Solid State Disk |
| SST | Solid State Transformer |
| TDCs | Traditional Data Centers |
| TPU | Tensor Processing Unit |
| TUPS | Traditional UPS |
| VRT | Voltage Ride Through |

Sina Mohammadi, Marcus Chen I Wada, Rouzbeh Haghighi, Ali Hassan, Hualong Liu and Wencong Su are with the Department of Electrical and Computer Engineering, University of Michigan-Dearborn, Dearborn, MI 48128 (e-mail: sinamo@umich.edu; wadamc@umich.edu; haghighi@umich.edu; alihssn@umich.edu; hualongl@umich.edu; wencong@umich.edu).

Wayne Wang, Archit Bhatnagar and Ang Chen are with the Department of Computer Science and Engineering, University of Michigan-Ann Arbor, Ann Arbor, MI 48109 (e-mail: wswang@umich.edu; architb@umich.edu; chenang@umich.edu). (corresponding authors: Wencong Su and Ang Chen)

## I. INTRODUCTION

Artificial Intelligence (AI) has fundamentally altered society's relationship with technology; spanning applications from simple search tasks to advanced scientific discovery. Large language models (LLMs) have been at the forefront of these high-complexity AI systems, with models such as ChatGPT and Claude, increasingly embedded in everyday use across the United States. These large-scale models are trained on trillions of text tokens collected from online sources and are deployed through web-based platforms that can attract millions over short periods of time. The surge in demand has prompted AI industry stakeholders to consider contemporary data center (DC) designs capable of supporting the high-computational tasks required for training, inference, and fine-tuning of increasingly more complex models. Energy requirements for AI queries are now nearly an order of magnitude greater than those of Google search, while AI training workloads have been observed to double approximately every 3.4 months [1]. Collectively, these trends highlight the necessity for rethinking data center architectures to sustainably support the rapid scaling of AI workloads.

DCs are dedicated facilities, or collections of facilities, designed to house computational systems, telecommunications equipment, and data storage infrastructure. Energy demand within a DC is unevenly distributed: IT equipment and cooling systems account for the majority of electricity consumption, while auxiliary loads such as lighting and security represent a comparatively small fraction [2]. Traditional data centers (TDCs) have historically operated at total power levels typically below 30 MW [2], with individual electrical distribution branches commonly limited to a few tens of kilowatts. These facilities are predominantly connected to power distribution networks in densely populated areas and operate under an architectural paradigm that emphasizes redundancy and exceptionally high uptime, making uninterrupted power delivery from the utility grid essential. TDCs are often sited near population centers to minimize latency for end users.

In contrast, AI DCs are driven by compute-intensive workloads, the widespread deployment of power-hungry GPUs, and the use of high-efficiency cooling technologies, all of which significantly increase power requirements. Thus, large-scale AI training facilities are increasingly located in remote or semi-rural regions where land, power, and cooling resources are more accessible and cost-effective. Rack-level power demand in AI DCs can exceed 100 kW, while aggregate facility consumption may scale to hundreds of megawatts or even gigawatt levels [3]. As a result, large-scale AI training facilities often require direct interconnection with transmission networks and face more strict reliability, siting, and environmental constraints than traditional facilities [4]. Inference-oriented facilities, while potentially smaller in individual footprint, may connect at either distribution or transmission level depending on aggregate scale and siting.

Beyond the differences in scale and infrastructure, AI DCs exhibit two distinct load profiles (training and inference) that differ fundamentally from those of TDCs. AI training workloads are characterized by rapid power fluctuations arising from idle periods, peak utilization events, and checkpointing operations, with significant load variations occurring on sub-second timescales. In addition, training jobs often produce high-frequency, jitter-like power spikes. In contrast, inference workloads generally lack such rapid transients and exhibit comparatively smoother demand profiles. TDC loads, by comparison, behave more like conventional grid loads and are typically predictable using historical data and standard forecasting methods.

AI DCs are connected to the power grid through high-density power converters, which lead to higher power distortion at the utility level. Besides, jittery spikes in training jobs may cause sub-frequency mechanical oscillations in synchronous generators, which increase mechanical stress and accelerate corrosion. As a result, harmonic compensation and load smoothing become a critical requirement for AI DC operation, both to improve load predictability and to mitigate adverse power-quality impacts on the power system.

Large-scale AI DCs enforce the power grid to accommodate higher reserve margins and proactive resource planning. This is because forecasting their load dynamics is more challenging than for traditional loads, and the uncertainty associated with these types of loads is significantly higher. Therefore, additional reserve capacity is necessary to maintain normal grid operation and to support grid expansion when integrating AI DCs.

Connecting or disconnecting large-scale AI DCs may jeopardize system stability due to high-range frequency fluctuations. These facilities are designed to rapidly transfer to backup power in response to even minor grid disturbances, which can trigger large, sudden load drops at the transmission level. Such disturbances may activate load-frequency relays or enforce grid operators to implement load-shedding scenarios. A recent transmission fault in Virginia triggered an abrupt 1,500 MW reduction in system load as multiple DCs transitioned to backup power, leading to significant frequency and voltage deviations that required operator intervention [5]. Events such as this illustrate the limitations of conventional grid planning and operational strategies when accommodating large AI DC loads.

Considering the above-mentioned challenges, we investigate on the role and impact of energy storage systems (ESSs) in enabling the smooth integration of future large-scale AI DCs into the power system. To the best of our knowledge, there is no comprehensive document specifically focusing on the potential support roles of ESSs in the reliable integration of AI DCs with the power grid. In this paper, we address this gap and investigate the role of ESS in AI DCs. ESSs can act not only as backup units with limited uptime but also support cooling through thermal storage units. They can be deployed as battery backup units (BBUs) inside IT racks, GPU-level batteries for chip-level load smoothing, and battery energy storage systems (BESSs) for DC-level load smoothing or co-generation support. ESSs within UPS systems can also interact with the utility grid to provide services such as frequency regulation and peak shaving. Fuel cells (FCs) are also have the potential to replace diesel back-up generation with technology advancements.

In contrast to [6], [7], this paper is highly focused on the role of ESSs in enabling reliable grid integration of AI DCs, rather than only characterizing the grid impacts of these large loads. Moreover, our work does not focus on ESS chemistry technologies [8], [9], but instead attempts to reveal design architectures for the optimal application of ESSs in AI DCs

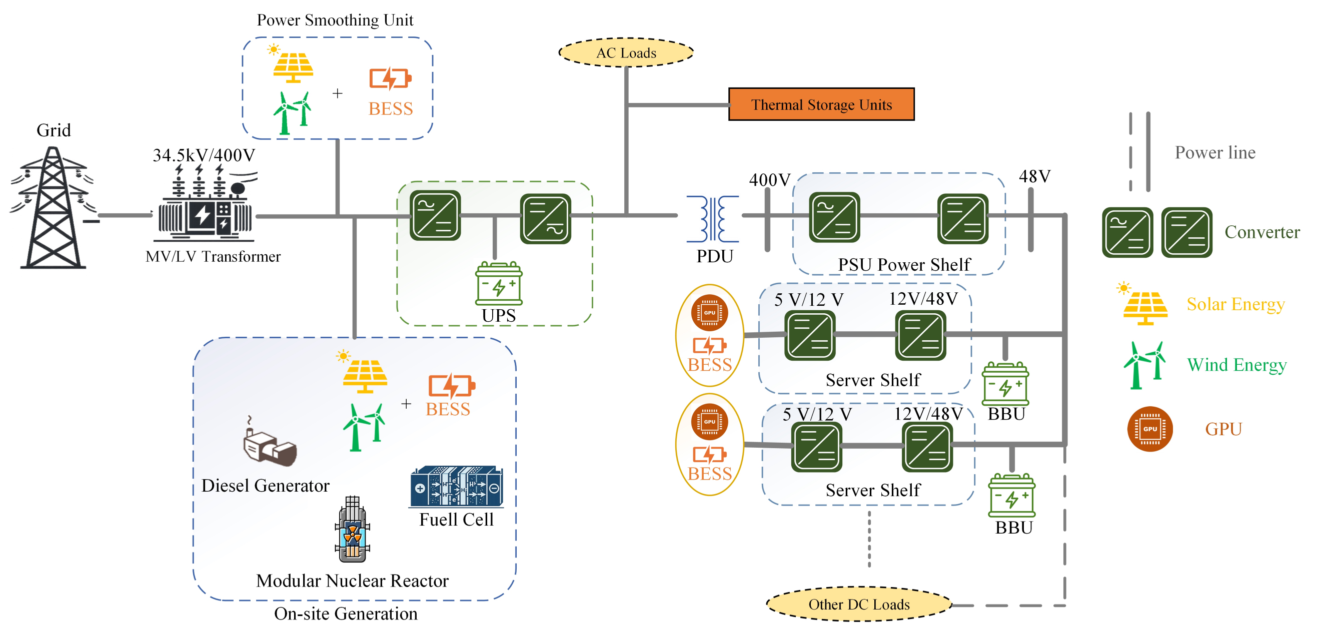


grid integration. Therefore, this study serves as an appropriate source for both academic and industry partners seeking the required knowledge to explore new avenues for the role of ESSs in future AI DCs.

The remainder of the paper is organized as follows. Section II provides an overview of the AI DC architecture, where IT equipment, power delivery systems, cooling systems, and miscellaneous units are examined, along with the required upgrades compared to TDCs. Section III investigates the role and operation of UPS systems, with particular emphasis on the grid-interactive UPS (GiUPS) systems, which has recently been studied as a key component of future AI DCs. Section IV discusses the integration of BESSs with AI DCs and their role in power smoothing and reliable grid integration, with a special focus on large-scale units. Sections V and VI address FCs and thermal energy storage (TES) systems, respectively, as non-battery-based energy storage solutions, highlighting their contributions to low-carbon on-site generation and more efficient cooling systems while maximizing the utilization of renewable energy sources (RESs). The role of rack-level and server-level ESSs is also examined as primary components for mitigating chip- and server-level power fluctuations, and their coordination requirements are emphasized in section VII. Section VIII investigates the role of second-life BESSs (SLBESSs) as cost-effective ESSs within the AI-DC architecture, and presents evidence demonstrating their capability to support centralized BESSs in AI DCs. Finally, Section X discusses the challenges associated with integrating multi-layer ESSs and outlines potential future research directions.

## II. AI DC Power Architecture

The AI DC infrastructure comprises different sections, including IT equipment, power distribution networks, cooling systems, and miscellaneous units such as lighting and security. In this section, we provide a brief introduction to the AI DC components and the ESS units in its structure. The overall structure of the AI DC with all ESSs is provided in Fig. I.

### A. *IT equipment*

The IT equipment itself comprises high-performance computational electronic chips such as GPUs, TPUs, and CPUs. It also includes advanced storage architectures, such as solid-state storage units, for storing required information with very high speed and efficiency. In addition, it considers resilient and secure networking among all processing units in AI DCs. High-speed, low-latency communication among AI accelerators is primarily achieved through Remote Direct Memory Access (RDMA) fabrics allowing direct memory-to-memory data transfers between nodes without CPU involvement. Dominant implementations include RoCEv2/InfiniBand across racks in training clusters [10] and direct GPU-to-GPU communication within racks via NVLink [11].

*1) Computing Units:* The computing unit consumes half of the required electricity of an AI DC [12]. NVIDIA GPUs such as H100, B200, or Blackwell Ultra have been used for training jobs in hyperscale AI DCs. For instance, the B200 utilizes 208 billion transistors that can be parallelized through very fast communication settings such as NVLink [13]. In addition, new GPU designs such as the GB300 NVL72 enable chip-level power smoothing using ESS [14]. Beyond NVIDIA, major cloud providers have developed custom AI accelerators optimized for their infrastructure: Google's Tensor Processing Units (TPUs) [15] are used to train and serve models such as Gemini, while AWS Trainium and Inferentia chips provide training and inference acceleration, respectively, enabling cloud-scale AI services.

AMD has also entered the AI accelerator market with its Instinct GPU series (e.g., MI300X), which offers competitive performance-per-watt for LLM training and inference workloads. These GPUs integrate CPU and GPU compute with high-bandwidth memory (HBM) in a unified package, positioning it as a direct competitor in hyperscale AI DCs. In section VII, the role of ESSs for power smoothing will be discussed in more detail.

*2) Data Storage Units:* AI training workloads place extreme demands on storage infrastructure, requiring high-throughput, low-latency access to datasets that can reach petabyte scale. NVMe SSDs have become the dominant storage medium in modern AI DCs, replacing both HDDs and legacy SATA SSDs due to their superior bandwidth and latency characteristics. HDDs, while still present in archival or cold-storage tiers of some traditional facilities, are largely absent from the hot data path in AI training environments, where even brief I/O stalls can idle expensive GPU clusters [16].

The prevailing architectural trend in hyperscale AI DCs is *disaggregated storage*, in which compute (GPU servers) and storage are decoupled into independent resource pools interconnected via high-speed RDMA fabrics. Unlike traditional server-attached storage, disaggregation allows compute and storage capacity to scale independently, improves overall resource utilization, and enables storage to be shared across multiple training jobs simultaneously [10]. In practice, GPU servers access remote NVMe devices over RDMA-capable networks using protocols such as NVMe over Fabrics (NVMe-oF), achieving latencies that approach those of locally-attached storage. NVIDIA's GPUDirect Storage extends this further by enabling direct DMA transfers between NVMe storage devices and GPU memory, bypassing the CPU and host memory entirely and reducing both latency and CPU overhead for I/O-bound training workloads [17].

*3) Networking:* AI DCs aggregate thousands of GPU accelerators into tightly coupled parallel training clusters, placing extraordinary demands on the underlying network fabric. Unlike TDCs, where network traffic patterns are largely client-server in nature, AI training workloads generate dense all-to-all communication patterns during gradient synchronization across distributed model replicas. This requires network fabrics that deliver high bandwidth, ultra-low latency, and minimal congestion at scale [10].

The foundational transport mechanism in modern AI DC networks is RDMA, which enables direct memory-to-memory transfers between nodes without CPU involvement, reducing both latency and CPU overhead. While InfiniBand has historically been used in HPC settings and remains present in some training clusters, the industry has broadly converged on RoCEv2 (RDMA over Converged Ethernet) [18] as the fabric of choice at hyperscale, offering comparable performance over commodity Ethernet switching infrastructure at lower cost and with greater operational flexibility [10], [19]. NVIDIA's Spectrum-X platform is specifically engineered to optimize RoCEv2 performance for AI workloads, addressing congestion control and load balancing challenges that arise in large-scale training deployments [19].

Within a single node or rack, inter-GPU communication bypasses the network fabric entirely through NVIDIA NVLink, a high-bandwidth direct interconnect that enables GPU-to-GPU data transfers at bandwidths far exceeding those achievable over any network interface [11]. Beyond a single rack, scale-out communication relies on the RDMA fabric described above.

### *B. Power Delivery Systems*

The power delivery systems in an AI DC contain the external utility grid, internal power distribution, UPS, on-site backup generation, and the associated control systems.

*1) External Utility Grid:* TDCs, with power consumption on the order of a few megawatts, can typically be directly connected to distribution grids at voltage levels such as 34.5 kV or 13.2 kV. However, hyperscale AI DCs, requiring more than 100 MW of power, should be connected to transmission grids to ensure reliable and stable grid operation [2]. However, there is no standardized voltage level across utilities for integrating large loads such as AI DCs. The utility power is then transformed to a lower voltage level through a medium-voltage to low-voltage distribution transformer, typically 480 V, to feed the internal power distribution within the DC. This transformer also electrically isolates the AI DC from the grid. The 480 V AC is then distributed among the various components of the AI DC, including the UPS system, power distribution units (PDUs), cooling system, and IT equipment.

*2) UPS system:* The UPS system is comprised of an AC-to-DC power converter, a battery storage unit, and a DC-to-AC power converter. Power is stored in the storage unit under normal conditions, and the stored energy is used during emergency conditions when there is a loss of utility power or rapid fluctuations that jeopardize the normal operation of IT loads. In TDCs, UPS operation is typically limited to a few seconds, after which on-site generation units take responsibility for powering the DC in the absence of utility power for several hours.

The UPS requirements for AI DCs differ significantly from those of TDCs. The UPS system for AI DCs should operate over different ranges, including short-, medium-, and long-duration operation. Medium- and long-duration operation provides more time for on-site generation activation or, in some cases, can eliminate the need for separate backup units. GiUPS systems with high power density and large storage capacity can also be implemented to enable grid-support functions, including peak shaving or frequency regulation scenarios. The UPS systems in modern AI DCs will be discussed in detail later in Section III.

*3) Backup On-Site Generation:* Backup generation units are utilized in DCs to provide electrical power under emergency conditions when utility power is unavailable. Backup generation is activated a few seconds after a utility power interruption, following the UPS response. Diesel backup generators are used in TDCs because they are combustion-based units that can provide a fast response; however, they are not environmentally friendly. RESs with appropriate BESSs can also be utilized for backup generation, as discussed in more detail in Section IV. However, power density, implementation cost, and the required space for installing PV panels or wind turbines are challenging issues in this context [20]. Modular nuclear reactors have also recently been introduced for AI DCs, offering MW-level power generation [21]. The technology for this type of equipment is still immature, implementation costs are high, and spent nuclear fuel must be stored properly. In addition, FCs may be better options for backup generation, as they can provide high power with fast response. Moreover, the development of hydrogen-based FCs can enable clean generation units within AI DCs [22]. The role of FCs in backup generation for future AI DCs will be discussed thoroughly in Section V.

### C. Cooling Systems

The IT equipment inside a DC produces heat as a result of electrical losses within electronic chips. As the computational power and power density of computing units increase, the associated losses and heat generation also increase. In AI DCs, due to the presence of high-intensity AI accelerators, advanced cooling systems are required to enhance IT load performance and optimize power consumption. In TDCs, air is used as the primary medium for cooling IT equipment. Chilled air is injected into server rooms, and the temperature is maintained at a certain level using a central cooling controller. Air-cooling systems are cost-efficient, reliable, and agile. They can be easily extended to larger facilities, and the required hardware can be modified quickly. However, the efficiency of air-cooling systems is low for effectively cooling power-hungry AI accelerators.

Liquid cooling is a more advanced cooling system developed for AI DCs. By utilizing liquid cooling systems, cooling can be provided at the rack level or even at the chip level. Liquid cooling offers better heat transfer, requires less energy and space, and is more efficient compared to air-cooling systems. It also eliminates the need for large mechanical fans, which are less reliable. Direct-to-chip cooling circulates a dielectric liquid through cold plates into chips and processing units and can efficiently dissipate heat [23]. Hybrid cooling systems combine the agility of air cooling with the efficiency of liquid cooling, making them a suitable option for hyperscale AI DCs where redundancy can be achieved through hybrid solutions.

TE units can also be utilized in parallel with different types of cooling systems [24]. The TEs absorb chilled air or water and inject it into the IT equipment at specific times. Utilizing TEs can effectively increase efficiency in AI DCs. TEs cool the air or liquid by accessing extra energy from on-site generation units during normal DC operation. The role of TEs as cooling system accelerators in future AI DCs will be discussed thoroughly in Section VI.

### D. Miscellaneous Units

Apart from IT equipment, power delivery, and cooling systems, there are other units required for the normal operation of AI DCs. These include the physical infrastructure for housing servers, racks, and wiring systems, as well as the lighting system within the AI DCs. In addition, security and control rooms are also integral units of a AI DC. Miscellaneous units in an AI DC consume significantly less electricity than the other sections.

## III. UPS Systems in AI DCs

### A. Traditional UPS (TUPS) Operation and Limitations

UPS systems are fundamental components in AI DCs, ensuring continuous operation of critical loads during grid disturbances or outages. Conventional UPS systems [25], [26],

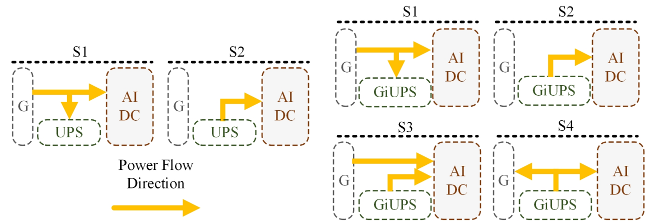


Fig. 1. UPS and GiUPS operation modes

[27] typically operate in standby or online modes. In standby mode, the UPS remains bypassed during normal operation and transfers to battery-supported inverter operation only when a disturbance is detected. In online mode, the rectifier and inverter continuously process power, providing isolation from grid disturbances and maintaining tight voltage and frequency regulation at the critical bus (see Fig. 1). In both modes, the UPS interacts with the grid only through battery charging and synchronization. The UPS is therefore treated as a passive protective device.

### B. GiUPS systems in AI DCs

TUPS architectures were designed primarily for load protection with minimal interaction with the utility grid. This paradigm is increasingly insufficient for AI DCs. First, AI workloads introduce rapid load variations that propagate upstream and cause voltage flicker, transformer thermal stress, and feeder congestion [28]. These effects are amplified when multiple AI racks operate in synchrony, which is common in distributed training. Second, the growing penetration of renewable energy reduces system inertia and increases the rate of change of frequency. TUPS systems do not contribute to frequency support beyond simple ride-through, which leaves a large amount of inverter capacity unused during normal operation [29]. Third, the energy stored in UPS batteries remains idle for more than 99 percent of their lifetime, representing a significant opportunity cost. These limitations motivate the development of UPS architectures capable of dynamic grid interaction.

GiUPS systems enhance TUPS designs by incorporating bidirectional power converters, advanced digital controllers, and communication interfaces that allow coordination with the utility grid or market operator. These systems can modulate active power in response to grid frequency deviations or dispatch signals, enabling participation in services such as primary frequency regulation, fast frequency response, synthetic inertia, and peak load management [30], [31], [32]. Unlike TUPS systems, which operate independently of grid conditions except during outages, GiUPS systems continuously monitor grid conditions and adjust their output accordingly.

GiUPS can provide fast frequency response (FFR) within 0.5 to 10 seconds after a grid event. It can operate in a dynamic frequency response mode. In this mode, the injected battery power is adjusted in real time based on frequency regulation needs. The UPS can also operate in a static frequency response mode. In this case, a fixed amount of power is injected after a grid event such as a fault or large load switching [33].

TABLE I
OVERVIEW OF GIUPS OPERATING MODES

| Mode | Grid Input | Battery Output | Trigger Condition | Key Feature |
|---|---|---|---|---|
| Standard Operation | 100% | 0% | Normal operation | Standard double-conversion UPS |
| Discharge-Full Disconnection | 0% | 100% | External command | Fully battery-powered load |
| Discharge-Partial Disconnection | $<$100% | Partial (e.g., 25%) | External command | Mixed grid and battery supply |
| Recharge | Supply $>$ Load | Battery charging | SOC $<$ 100%, over-frequency | Power limited (20–25% of UPS capacity) |
| Energy Export | Adjustable | Discharge to grid | Regulatory approval | Bi-directional power conversion |

*1) Operational Modes of GiUPS:* GiUPS can operate in several modes depending on the grid conditions and external control signals, including *standard operation*, *discharge modes* (full and partial disconnection), *recharge mode*, and *energy export (bi-directional) mode* [30], [34]. When a frequency variation is detected by an external controller, the GiUPS adjusts its operation to provide both positive and negative regulation by charging or discharging its batteries within operational limits. Table I, shows an overview of GiUPS operation modes.

Under normal conditions, the GiUPS receives 100% of the input power from the utility grid through the rectifier, delivering it to the load (see S1 in Fig. 1). In this mode, the GiUPS functions as a standard double-conversion system, with the batteries maintained in standby and not actively supplying power. This operation is referred to as the *standard UPS operation*.

Discharge modes are employed to meet external control requests, supplying energy to the load or the grid. In the *full disconnection mode*, the GiUPS is completely disconnected from the utility, and 100% of the load power is supplied by the batteries (see S2 in Fig. 1). In the *partial disconnection mode*, the input power from the grid is reduced according to external commands, with the remaining load power supplied by the batteries (see S3 in Fig. 1). For example, the batteries may provide 25% of the total load power while the grid supplies the remainder.

When the battery state of charge (SOC) is below 100% (e.g., 80%) and an over-frequency event is detected, the GiUPS draws power from the grid to recharge the batteries. This operation is referred to as *recharge mode*. The maximum recharge power is typically limited to 20–25% of the GiUPS nominal capacity, constrained by battery recharge characteristics and the maximum input current.

The GiUPS can also operate as a bi-directional power converter to inject energy back into the grid (see S4 in Fig. 1). This *energy export mode* is subject to local regulatory and grid requirements and allows the GiUPS to discharge batteries upstream.

*2) GiUPS Reactive Power Support and Voltage Ride-Through (VRT) Capability:* In addition to active power modulation, advanced GiUPS systems can provide reactive power injection and VRT capabilities, which are increasingly required by modern grid codes and interconnection standards [35], [36]. Reactive power support is enabled by the bidirectional inverter stage, which can independently regulate active and reactive current components under a synchronous reference frame control strategy. GiUPS units typically provide reactive power capability in the range of 20–40% of their rated kVA. For example, a 1 MW/1.1 MVA GiUPS can supply approximately $\pm$250–300 kVAr of dynamic reactive support. GiUPS can inject or absorb reactive power without significantly affecting active power delivery to the critical load. This capability allows the DC to contribute to feeder voltage regulation, mitigate voltage fluctuations caused by rapid AI load variations (often inducing 5–10% voltage swings within milliseconds), and improve local power factor at the point of common coupling (PCC) from typical values of 0.92–0.95 to above 0.99 [37], [35].

VRT capability ensures that the GiUPS remains connected and operational during short-duration voltage sags or swells [38]. TUPS systems typically transfer to battery mode during severe disturbances, effectively isolating the load from the grid. In contrast, GiUPS systems are designed to comply with low-voltage ride-through (LVRT) and high-voltage ride-through (HVRT) requirements, similar to grid-scale inverter-based resources. Typical LVRT profiles require the inverter to remain connected down to 0.2 pu for 100–150 ms, and down to 0.5 pu for up to 500 ms. During a voltage sag, the GiUPS can increase reactive current injection proportionally to the voltage deviation, often delivering 2–3 pu reactive current within 2–5 ms, thereby supporting grid voltage recovery while maintaining uninterrupted supply to the critical load.

The coordination between active power support, reactive power regulation, and VRT functionality requires a hierarchical control framework [39], [40], [41]. In grid-following (GFL) mode, the GiUPS synchronizes to the grid using a phase-locked loop (PLL) and provides reactive current according to predefined droop characteristics (typically 3–5% voltage droop) or grid operator commands. In grid-forming (GFM) mode, the inverter can regulate terminal voltage magnitude and frequency directly, enabling seamless transition to islanded operation if grid conditions deteriorate beyond acceptable thresholds. Protection logic ensures that grid support functions never compromise critical load reliability, maintaining load voltage within $\pm$1–2% even during external disturbances.

*3) GiUPS Topologies:* For GiUPS applications, topologies that support bidirectional power flow and high-speed digital control are preferred. Double-conversion and delta conversion architectures with bidirectional converters can rapidly transition between load-following, grid-support, and islanded operation. Modular architectures are particularly attractive in AI DCs because they allow some modules to participate in grid services while others remain dedicated to critical load protection. This partitioning reduces operational risk and improves economic performance [30]. Emerging DC-coupled architectures further reduce conversion stages and improve round-trip efficiency. These architectures also enable direct coupling with on-site renewable generation or FCs, which enhances the ability of the AI DCs to operate as controllable grid resource.

### C. BESS Sizing in GiUPS Systems

The sizing of the BESS in GiUPS applications must simultaneously satisfy backup reliability requirements and grid-service performance objectives [7], [8]. GiUPS participation in services such as FFR, primary regulation, and peak shaving introduces additional sizing considerations. Frequency regulation is primarily power-intensive rather than energy-intensive, requiring high ramp rates and short-duration injections. Consequently, the inverter power rating may approach the full UPS capacity even if incremental energy capacity beyond backup requirements remains moderate. Cycle life and cumulative energy throughput are critical determinants of economic sizing. Grid-service participation may introduce hundreds of shallow cycles annually [42], [43], [44], [45]. Battery degradation correlates strongly with equivalent full cycles, temperature, and average state of charge [46], [47], [48], [49]. Moderate oversizing of the BESS can reduce effective depth of discharge (DOD) per cycle, extending service life and lowering long-term replacement cost. However, excessive oversizing increases capital expenditure, footprint, and thermal management complexity without proportionate revenue gains.

An optimal sizing methodology therefore integrates (i) backup energy constraints, (ii) committed grid-service power capacity, and (iii) degradation-aware lifecycle cost modeling. Optimization frameworks typically minimize total cost of ownership while ensuring reliability margins and projected ancillary service revenues. For AI DCs with highly dynamic loads, an additional allocation of BESS capacity may be reserved for short-term load smoothing to mitigate upstream ramp rates and transformer stress. This buffering function must be explicitly included in sizing calculations to prevent erosion of guaranteed backup autonomy. This further highlights the role of long-duration ESSs (LDESSs) in modern UPS systems, which are currently under investigation for grid use cases.

## IV. BESS IN AI DCS

BESS integrated with DCs represent a practical and scalable solution to address the challenges imposed by large and highly dynamic loads on the power system [50]. When appropriately designed and controlled, BESS can play a critical role in mitigating large load fluctuations, enhancing local power quality, and supporting overall grid stability [12]. To establish a clear understanding of the underlying mechanisms and achievable benefits, this section reviews the fundamental BESS control paradigms, with emphasis on grid-forming and grid-following modes of operation. The discussion then extends to key grid-support functions enabled by AI DC–connected BESS, including co-generation, power smoothing and frequency regulation. Finally, the cost and sizing implications of BESS deployment are examined.

### A. BESS Control Modes

From an operational perspective, AI DCs can be configured for grid-tied or islanded operation, depending on the BESS inverter control mode and the facility-level coordination architecture. GFM control enables the BESS to establish the voltage and frequency reference required for islanded operation. In grid-tied mode, the BESS can charge or discharge to support peak shaving and increase renewable self-consumption, whereas in islanded mode it serves as the anchor resource to supply the AI DCs and potentially reduce reliance on conventional generation or support renewable co-generation [51], [52].

*1) GFM Control Model:* In grid-forming operation, the BESS behaves as a controlled voltage source and establishes its own internal frequency and phase without relying on an external phase-locked loop (PLL) [53]. The controller emulates the swing dynamics of a synchronous generator by incorporating virtual inertia, damping, and active power–frequency droop characteristics.

The inverter angle dynamics are given by

$$\frac{d\delta_{\mathrm{vsm}}}{dt} = \omega_{\mathrm{vsm}}, \tag{1}$$

while the internal frequency dynamics are described by

$$2H_{\mathrm{vsm}}\frac{d\omega_{\mathrm{vsm}}}{dt} = P_{\mathrm{ref}} - P - \left(\frac{1}{m_p} + D_1 + \frac{sD_2}{s+\omega_D}\right)(\omega_{\mathrm{vsm}} - \omega_0)\,. \tag{2}$$

Here, $H_{\mathrm{vsm}}$ is the virtual inertia constant, $m_p$ is the active power–frequency droop coefficient, $D_1$ represents steady-state damping, $D_2$ is a transient damping term shaped by a washout filter with corner frequency $\omega_D$, $\omega_{\mathrm{vsm}}$ is the inverter angular frequency, $\omega_0$ is the nominal angular frequency, $P_{\mathrm{ref}}$ is the active power reference, and $P$ is the measured inverter output power. This formulation enables autonomous frequency regulation and inertial response, making GFM BESSs suitable for islanded operation [54].

*2) GFL Control Model:* In contrast, GFL BESS operate as controlled current sources that synchronize to an externally imposed grid voltage using a PLL [55]. The inverter frequency and phase are therefore dictated by the grid rather than internally generated.

A conventional synchronous-reference-frame PLL can be expressed as

$$\omega_{\mathrm{pll}} = \omega_0 + K_p v_q + K_i \int v_q \, dt, \tag{3}$$

$$\frac{d\delta_{\mathrm{pll}}}{dt} = \omega_{\mathrm{pll}}, \tag{4}$$

where $v_q$ is the quadrature-axis component of the measured grid voltage in the PLL reference frame, $K_p$ and $K_i$ are the proportional and integral gains of the PLL, and $\delta_{\mathrm{pll}}$ and $\omega_{\mathrm{pll}}$ denote the estimated grid angle and frequency, respectively.

Because GFL inverters depend on a strong external voltage reference, their performance degrades under weak-grid conditions, motivating the adoption of GFM control strategies in inverter-dominated systems [54].

The BESS terminal-voltage dynamics $E$ are modeled as

$$k_{iv}\frac{dE}{dt} = V_{\mathrm{ref}} + m_q\left(Q_{\mathrm{ref}} - Q\right), \tag{5}$$

where $k_{iv}$ is the integral gain, $V_{\mathrm{ref}}$ is the voltage reference, $m_q$ is the $Q$–$V$ droop coefficient, $Q_{\mathrm{ref}}$ is the reactive power reference, and $Q$ is the measured reactive power. This formulation regulates the inverter voltage magnitude through a reactive-power droop relationship.

TABLE II
SUMMARY OF POWER-SMOOTHING ARCHITECTURES FOR AI DATA CENTERS: BENEFITS AND CHALLENGES [56]

| Architecture | Benefits | Challenges |
|---|---|---|
| Advanced GFM + GFL BESS Solution | • Load smoothing/shaping<br>• Demand flexibility<br>• Grid services<br>• Lower cost and footprint | • Complex control strategy<br>• Fast measurement and communication<br>• Advanced plant-level control |
| Hybrid E-STATCOM + BESS Solution | • Load smoothing and/or shaping<br>• Demand flexibility<br>• Grid services<br>• Lower flicker | • Higher cost<br>• Increased footprint<br>• Control interaction |
| Grid-Forming BESS | • Load smoothing/shaping<br>• Demand flexibility<br>• Support grid services/stability | • May require a line reactor<br>• Higher flicker<br>• Plant-level control |
| Supercapacitors (e.g., E-STATCOM) | • High-speed response<br>• Effective load smoothing/shaping<br>• Reduced flicker | • POI demand management<br>• Not supporting grid services<br>• Does not offer GFM support |

### *B. Grid Support Roles of BESS in AI DCs*

*1) On-Site Clean Power Integration:* BESS play a critical role in enabling RESs integration at AI DCs. Given the energy-intensive nature of AI DCs, on-site renewable generation and off-site procurement mechanisms such as power purchase agreements (PPAs) are increasingly adopted to reduce operating costs and meet sustainability objectives. However, the inherent intermittency of renewable resources complicates reliable power supply. BESS mitigate these challenges by storing excess energy during periods of high generation and supplying it during low availability, while also providing backup power, and improved renewable utilization [57]. AI DC–integrated BESS can be architected either as large, multi-megawatt GFM resources capable of replacing conventional backup generators, or as large-capacity batteries integrated within static UPS systems [58]. In this context, GiUPS systems, traditionally designed for short-duration ride-through, are increasingly complemented by dedicated BESS that are optimized for extended energy management and grid-interactive operation rather than transient backup alone [52]. At the converter-control level, BESS can be configured for GFM, GFL, or hybrid GFM and GFL operation to balance fast dynamic response, voltage/frequency support, and grid-service capability, although with added control and sensing complexity.

*2) Power Smoothing:* BESS can inject or absorb power at the facility interface to attenuate rapid AI DC demand variations and present a smoother power profile to the grid. A BESS co-located with an AI DC can provide grid-level power smoothing while supplying sufficient energy capacity to support sustained mitigation actions. This architecture improves operational reliability by enabling load shaping, demand flexibility, and extended ride-through for AI workloads.

As shown in Fig. 2, the GFM BESS effectively smooths the power fluctuations of the AI DCs resulting from training and inference jobs. An alternative approach is a hybrid E-STATCOM and BESS configuration, which combines the fast, high-speed charge/discharge response of supercapacitors with the higher energy capacity of BESS to achieve effective smoothing and sustained load support. This hybrid architecture can enhance resilience by improving demand flexibility, reducing flicker, and enabling broader grid-service capability. The primary trade-off is increased cost and footprint compared with standalone solutions. In addition, standalone supercapacitor-based E-STATCOM solutions can mitigate high-frequency AI load fluctuations and improve power quality for sensitive IT equipment by reducing flicker, although they provide limited long-duration energy support [56]. Table II compares the benefits and challenges of representative BESS-based and hybrid strategies for enabling grid support from AI DCs.

*3) UPS-Integrated BESS:* UPS-integrated BESS are motivated by a simple premise: AI DCs already deploy UPS systems with fast power-electronic interfaces, and augmenting this mandatory infrastructure with BESS enables grid-interactive capability with limited additional integration complexity. In practice, grid-interactive deployments also show that battery technology selection depends on the targeted services and operating constraints. For example, UPS-integrated BESS have been used to provide FFR by leveraging the rapid controllability of UPS power converters [58], [59].

The UPS-integrated BESS, labeled as *power smoothing units* in Fig. I, extend this concept by supporting long-duration outage operation and enabling participation in demand response programs, while the UPS maintains continuity of critical loads when neither the grid nor the BESS can fully supply

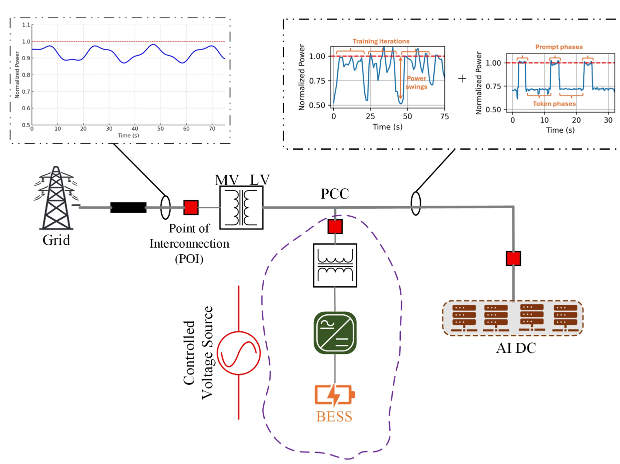


Fig. 2. GFM BESS as a power smoothing unit [56]

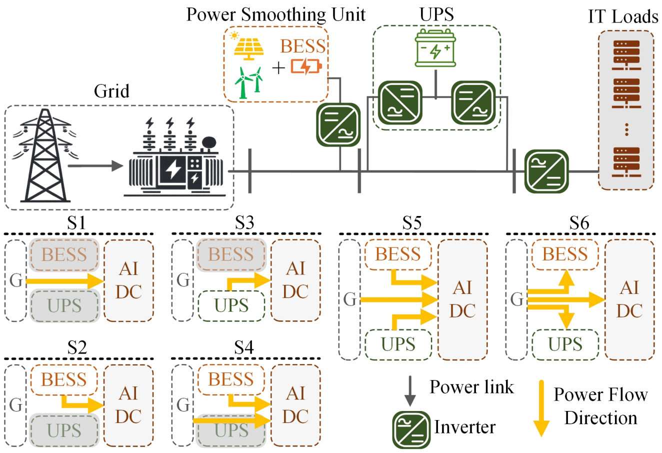


Fig. 3. UPS-Integrated BESS operation modes

demand. Although this architecture increases installation cost, it can significantly improve overall system reliability [31].

As summarized in Fig. 3, a GiUPS-integrated BESS can operate in (i) standard mode, (ii) discharge mode under full or partial disconnection, (iii) grid-services mode, and (iv) recharge mode for SoC recovery [30]. This architecture can reduce the need for bidirectional power flow across the MV/LV distribution transformer by localizing fast power exchanges, allowing the transformer to operate primarily under its normal unidirectional loading conditions [60]. These operating modes within the UPS–BESS subsystem enable long-duration BESS to enhance DC resilience through extended backup, reduce or eliminate reliance on diesel generation, participate in ancillary and reserve markets, manage demand charges and time-of-use tariffs, and increase RESs utilization [52].

*S1) Normal operation:* The AI DC load is supplied entirely from the utility grid, and the system delivers 100% of the input power to the AI DC.

*S2) Full disconnection with sufficient BESS reserve:* The site is fully isolated from the utility, and upon command from an external controller, the BESS supplies 100% of the AI DC load power. In this case, long-duration, large-scale BESS becomes essential; salt-cavern redox flow batteries are a promising due to their high safety, large storage capacity, stable temperature, and low cost [61].

During the transition from Scenario S1 to S2, the UPS initially supports the load because its response time is on the order of milliseconds, while the BESS typically requires a few seconds to assume full load supply. Once engaged, the BESS can sustain operation for extended durations (e.g., on the order of 1–4 hours, depending on sizing and operating conditions) [52].

*S3) Full disconnection with insufficient BESS reserve:* If the outage duration is long and the BESS does not have sufficient available capacity to supply the full AI DC load, the UPS assumes responsibility for supporting the critical load.

*S4) Partial disconnection:* The external controller reduces the grid input power, and the remaining portion of the AI DC demand is supplied by the BESS. This operating mode enables the BESS to support grid frequency regulation and to present a smoother power profile at the grid interface.

*S5) Coordinated UPS–BESS power smoothing:* The grid, BESS, and UPS jointly supply the AI DC load, with the UPS helping the BESS by providing fast support during critical transient conditions to assist power smoothing and frequency response. This case can be interpreted as an extension of S4 in which the UPS contributes rapid, short-duration buffering when required.

*S6) Recharge mode:* When the SOC drops below full charge, the utility initiates battery recharging (e.g., following an over-frequency detection). Under this condition, the UPS is prioritized for recharging first, after which the BESS can be recharged from the grid or from on-site renewable generation.

### C. BESS Cost and Sizing Considerations

The cost of BESS per kilowatt-hour has declined dramatically, dropping from approximately $7,500 in 1991 to $133 in 2024, with projections indicating a further reduction to around $80 by 2030 [52]. This downward cost trajectory is expected to continue with further scale-up in manufacturing capacity and advances in both manufacturing and battery recycling processes.

In addition to capital cost, effective sizing must account for operational objectives. Co-generation, power smoothing, and assisting GiUPS each require independent studies to determine the optimal BESS size. Sizing also affects the number of BESS units required for AI DCs. The sizing study will provide precise information on whether a single hyperscale BESS is more optimal than multiple grid-scale BESS units. Recent studies have applied advanced methods to determine the optimal BESS capacity while ensuring the required capacity and satisfying dispatch constraints [62], [63], [64]. Reference [65] shows that a 560 kWh Lithium-ion BESS, along with a 960 kWh lead-acid BESS, can provide FFR and backup power generation for TDCs. This study can be further extended to AI DCs as well, in which the cooperation between UPS and BESS is also considered.

In [62], an evolutionary algorithm is used to generate a Pareto front across different battery capacities, enabling selection of an appropriate size based on the desired balance between operational benefits and battery degradation impacts. In [63], the BESS capacity is determined using a bi-level optimization framework in which the upper layer searches for the optimal storage size that minimizes the total system cost. For each candidate size, the lower layer performs optimal microgrid operation, including data center, and the BESS capacity that yields the lowest combined investment and operational cost is selected. On the other hand, [64] has investigated the BESS sizing for a data center based on reliability requirements rather than cost optimization. The required storage capacity is obtained by estimating the minimum battery backup time needed to maintain uninterrupted operation under stochastic grid outages and generator failures.

## V. Fuel Cells (FCs) in AI DCs

FCs convert chemical energy directly into electrical energy through electrochemical oxidation reactions. Because this conversion is not combustion-based, FCs can achieve electrical efficiencies exceeding 60%, which is significantly higher than

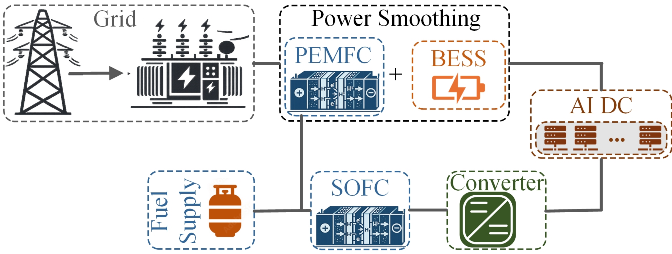


Fig. 4. FC integration with AI DC.

many conventional generators [66]. FC systems offer high operational reliability due to their modular design and minimal use of mechanical components, resulting in reduced maintenance requirements and high availability. When supplied with hydrogen, FCs produce no carbon dioxide or conventional air pollutants during operation [67].

Among the several established FC chemistries, Solid Oxide Fuel Cells (SOFCs), in context of AI DCs, are often highlighted for their high steady-state efficiency and suitability for long-duration on-site power generation [68]. Polymer Electrolyte Membrane Fuel Cells (PEMFCs) exhibit faster electrochemical response and greater compatibility with power-electronic interfacing, making them promising candidates for coordinated power smoothing [69]. As illustrated in in Fig. 4, both SOFC and PEMFC systems rely on a shared upstream fuel supply while serving distinct operational roles: SOFCs assist with base-load power to the AI DC, whereas PEMFCs, co-located with BESS, operate at faster timescales to mitigate short-term power fluctuations. With a consistent and reliable fuel supply, this architecture enables hierarchical coordination between the fuel infrastructure, on-site generation, and the utility grid.

### A. Role of FC in AI DCs

Commercial deployments, such as Bloom Energy's SOFC systems, despite their relatively high capital cost, have demonstrated the feasibility of FC installations capable of supplying primary or supplemental power to TDCs. These systems are typically configured to provide continuous or long-duration power, serving as low-emission and more energy-efficient alternatives to diesel generators [70]. In emerging AI DCs, whose power profiles are characterized by large, rapid, and highly synchronized load variations, FC-based technologies must be integrated within a broader energy architecture and operated as slow-following or baseload resources in order to preserve efficiency and lifetime. Accordingly, two complementary roles are considered:

*1) FC On-Site Generation:* SOFC-based systems are primarily suited for on-site generation in AI DC environments due to their high steady-state electrical efficiency, fuel flexibility, and scalability to megawatt-class power levels [68]. When supplied by pipeline natural gas or on-site hydrogen storage, SOFC systems can provide sustained power delivery over extended durations, making them alternatives to diesel generators for backup and resilience applications. Unlike battery-based systems, whose backup duration is limited by stored energy capacity, FC-based backup duration is primarily constrained by fuel availability, enabling outage coverage ranging from hours to multiple days depending on infrastructure configuration. However, due to their high operating temperatures and slow thermal dynamics, SOFC systems are not designed for rapid power modulation and are therefore best operated as baseload or slow-following generators within a coordinated energy management framework.

*2) FC-Assisted Power Smoothing:* PEMFCs operate at significantly lower temperatures than SOFCs and exhibit faster electrochemical response, enabling limited power modulation relative to high-temperature FC technologies. Experimental studies at the tens-of-kilowatt scale have demonstrated that PEMFC systems can achieve sub-second power ramping under carefully controlled conditions [71]. However, these studies also show that stack power extraction must be constrained by maximum allowable ramp rates to prevent fuel starvation, voltage collapse, and accelerated degradation. Repeated exposure to aggressive load transients has been associated with catalyst deterioration, membrane stress, and performance loss. Consequently, while PEMFCs may contribute to low-frequency power balancing service provision, they are not well suited to serve as primary resources for high-frequency load smoothing in AI DCs [72].

In practical deployments, PEMFC operation must, therefore, be coordinated with on-site BESSs and GiUPS systems. In such hierarchical architectures, BESSs and UPS systems regulate fast load transients and maintain AI DC-bus stability on millisecond-to-second timescales, while PEMFCs are dispatched through filtered power references that limit ramp rates and confine operation to degradation-aware regimes. Continuous monitoring of PEMFC operating conditions is essential both for degradation analysis and for coordinated control with fast-acting storage systems. When integrated in this manner, PEMFCs can complement BESS-dominated load smoothing strategies by supplying average power and extending overall system endurance without being subjected to damaging high-frequency load variations [69].

### B. Sizing Considerations

Scaling FC technologies to AI DC capacities introduces constraints related to physical aggregation, hydrogen logistics, and balance-of-plant complexity.

GFM control strategies for PEMFC systems have primarily been validated at the tens-of-kilowatt scale. Scaling such architectures to the multi-megawatt level requires parallel stack aggregation, coordinated hydrogen distribution manifolds, auxiliary subsystem synchronization, and high-capacity DC/DC and DC/AC conversion stages [73].

SOFC systems exhibit a distinct scaling trajectory. Hybridized configurations that integrate bottoming cycles for thermal energy recovery have demonstrated stable operation at multi-megawatt and hundred-megawatt scales [68]. In these installations, performance gains arise primarily from thermodynamic integration. As capacity grows, system complexity (increases) toward thermal management and mechanical integration.

Accordingly, sizing decisions for AI DC deployments should not be based solely on nominal power ratings, but on the interaction between electrochemical constraints, infrastructure requirements, and load temporal characteristics. PEMFC capacity, if deployed, should be bounded by hydrogen logistics and ramp-rate considerations, while SOFC capacity may be aligned with the steady baseload fraction of demand.

## VI. Thermal Energy Storage (TES) in AI DCs

TES refers to technologies that store energy in the form of heat or cold by raising or lowering the temperature of a storage medium relative to ambient conditions [74]. Unlike electrochemical and mechanical energy storage, TES does not directly support the electrical power, instead it reshapes the energy demand by decoupling thermal energy production from its consumption. This makes TES relevant in systems where thermal load are tightly coupled with performance and electrical demand, such as DCs [75].

In AI DCs, cooling constitutes 30-40% of total facility energy consumption [76] due to the high power density of accelerator-based computing. Nearly all electrical energy consumed by GPUs and associated IT equipment is ultimately converted into low-grade heat, with studies estimating that around 90 % of input electrical power manifests as waste heat within the DC environment [76]. Cooling demand, as a result, scales with computational load. While training DC power exhibits high-frequency power swings, thermal load evolves on slower timescales. This creates favorable conditions for the use of thermal energy storage to store cooling capacity and supply it during periods of high electrical demand or grid stress.

### A. Characteristics and Timescale of TES Operation

TES exhibits operational characteristics that differ fundamentally from electrical ESSs. Due to thermal inertia and heat transfer dynamics, these systems respond on slower timescales, typically ranging from several minutes to hours. As a result, TES is not suited for fast grid services such as frequency regulation or power quality support [77].

Instead, the storage units are well matched to applications involving load shifting, peak demand reduction, and ramp-rate mitigation of cooling-related electrical loads. Thermal standby losses and insulation constraints further limit the suitability of TES for long-term or seasonal storage in most data center applications. Consequently, TES is most effective when operated on diurnal timescales, complementing faster electrical storage technologies within a hierarchical energy storage framework [75].

### B. TES Technologies and Integration Architectures

*1) Sensible TES:* Sensible TES stores cooling capacity through temperature changes in a storage medium, most commonly water. Chilled water storage tanks are a mature and widely deployed form of the technology due to their simplicity, low cost, and ease of integration with conventional chilled-water systems [78]. However, because energy is stored through temperature differential rather than phase change, sensible TES exhibits comparatively lower volumetric energy density than alternative technologies. As a result, achieving equivalent storage capacity requires significantly larger physical volume and installation area.

Despite this footprint requirement, sensible water-based systems remain the least expensive option per unit of stored thermal energy and demonstrate predictable thermal behavior with minimal operational complexity [77]. For AI DC campuses where land availability permits, sensible TES provides a cost-effective and technically robust solution for short-term load shifting and peak chiller reduction.

*2) Latent TES (PCM-Based):* Latent TES exploits the phase change of materials to store thermal energy at nearly constant temperature. Compared to sensible storage, phase change materials (PCMs) provide higher volumetric energy density, allowing equivalent cooling capacity to be achieved with substantially reduced installation volume. This characteristic is particularly advantageous in space-constrained AI DC facilities [78].

The most widespread latent storage medium in cooling networks is ice, owing to its high latent heat and relatively low material cost. Ice-based TES has been successfully deployed in large-scale district cooling systems worldwide, demonstrating technical feasibility at substantial capacity [78]. However, latent systems introduce additional engineering complexity, particularly in heat exchanger integration, phase stability, and long-term cycling reliability. Although more compact than sensible storage, latent TES generally entails higher capital cost per unit of stored energy. Consequently, while ice-based TES offers clear volumetric advantages for cooling applications, its deployment in AI DC environments must balance footprint reduction against increased system complexity and economic uncertainty.

*3) Thermochemichal TES:* Thermochemical TES stores energy through reversible chemical or sorption processes, allowing thermal energy to be stored as chemical potential rather than as temperature change. Such systems can achieve high energy density and the lowest standby losses, making them attractive for long-duration storage [78].

Despite these advantages, thermochemical TES systems are generally complex, expensive, and less mature than sensible or latent storage technologies. Their application in DCs is currently limited to research and demonstration projects, though they represent a potential future option as cooling demands continue to increase.

### C. TES for RESs Integration

TES can support the integration of RESs in AI DCs by enabling power-to-cooling strategies. During periods of surplus RESs generation or low electricity prices, chillers can be operated to charge TES systems, storing cooling capacity for later use [79]. This approach improves the utilization of RESs and reduces reliance on grid power during peak or high-emission periods.

By shifting cooling-related electrical demand in time, TES enhances the flexibility of AI DCs as large grid-connected loads and supports broader decarbonization objectives.

## VII. Rack- and Server-Level ESSs roles in AI DCs

Rack- and server-level ESSs exist to handle two constraints that centralized UPS/BESS alone cannot satisfy: (i) *local*

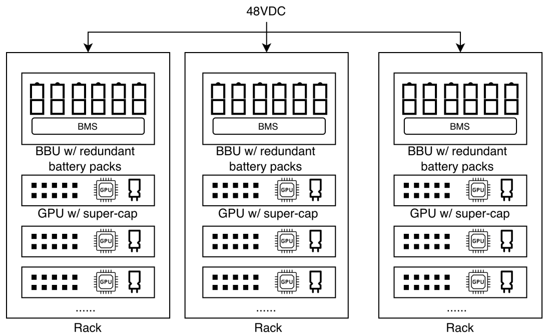


Fig. 5. Rack-level BBUs and server-level capacitors

*buffering* (GPU-/server-scale transients that require local energy buffering), and (ii) *fault domain* (limiting the blast radius of power disturbances and energy storage failures). In modern DC-architecture AI facilities, upstream layers (SST/MVDC front-ends and facility UPS/BESS) primarily set facility envelopes and ride-through at longer timescales, while downstream layers move buffering closer to the load to smoothen fast dynamics and localize contingencies under faults[80], [81]. This section focuses on rack-level BBUs as distributed ride-through and backup resources, and on server/GPU-level capacitive storage as power profile smoothening for the highest-frequency behaviors[82], [83], [84].

### A. Rack-Level ESS: Role, Benefits, and Constraints

The rack represents a natural operational and electrical boundary for AI infrastructure, with dense DC-architecture racks alone reaching MW-scale power demands [80]. Deploying energy storage at the rack level offers several advantages. First, the storage is electrically close to the load, enabling local buffering before propagating upstream to the facility distribution system. Second, failures in battery, converters, or wiring can be contained to individual racks, limiting the blast radius of faults. Third, storage capacity budgets and ride-through priorities can be configured on a per-rack basis, allowing workload-specific policies that reflect criticality differences across the DC.

Despite these benefits, rack-level deployment introduces operational challenges. Coordination becomes necessary, as many independent storage units must be managed for state-of-charge tracking, recharge scheduling, and availability monitoring. Safety and compliance requirements increase, since colocation of lithium-ion energy storage with IT equipment raises fire and thermal-runaway mitigation concerns. Finally, maintenance overhead grows substantially, as consistent monitoring, battery replacement, and preventive maintenance must be performed across racks. Fig. 5 shows the implementation of rack-level BBUs and server-level capacitors in the IT equipment.

### B. Battery Backup Units (BBUs) as Distributed UPS

In OCP Open Rack designs, BBUs are integrated into the rack as distributed DC ride-through modules that supply the rack DC bus during upstream AC disturbances [82]. In Open Rack V3 (ORV3) architecture, a BBU shelf typically hosts multiple BBU modules with $5{+}1$ redundancy and supports both *charge mode* and *discharge mode* operations with monitoring of SoC/SoH and maintenance tests [83]. Public reference designs summarize the intended operating point (e.g., per-module backup power on the order of kW for minutes, and lower-power charging over hours), reflecting a design goal of short ride-through and fast recovery rather than continuous power profile smoothening [85]. Meta reports ORV3 BBU shelves designed for minutes of backup, and notes that paired shelves can be used for higher rack power configurations [90].

*1) BBU vs centralized UPS:* BBUs and centralized UPS systems can both respond quickly in principle to supply the gap between grid power disturbance or outage and longer-term energy storage systems coming online (e.g., gensets / BESS), but they differ in *where* energy is buffered and *what* the buffer is optimized for. Centralized UPS concentrates energy and power conversion at room/facility scale, simplifying management and enabling grid-interactive use cases when permitted [34], [86]. Rack BBUs push storage behind fewer conversion stages in DC racks and reduce some double-conversion penalties compared to traditional centralized UPS architectures [89]. Practically, BBUs are best viewed as a distributed energy availability layer for the rack (seconds–minutes), not as the primary solution for sub-second smoothing which is handled more effectively by server/GPU capacitive buffers. Table III summarizes the high level comparison of rack-level BBUs and centralized UPS systems.

*2) BBUs as power absorbers:* BBU shelves inherently include charging control; in normal operation they remain in charge mode and can modulate charging current/power within design limits [82]. At hyperscale, uncontrolled simultaneous recharge can create step increases in aggregate load that trip upstream protection. Production case studies show that coordinated and priority-aware charging of distributed batteries can dramatically reduce recharge power (reported reductions up to $\sim$80%) while meeting recharge constraints [88].

However, using BBUs as a frequent, high-rate smoothing solution can accelerate degradation depending on cycling throughput, C-rate, SoC range, and temperature [87], [91]. Practically, server/GPU capacitors and software solution are better suited to handle high-frequency power fluctuation, and BBUs are better suited for ride-through, controlled recovery, and low-frequency shaping with budgeted cycling.

*3) Safety and deployment considerations:* Rack BBUs introduce Li-ion safety considerations near IT equipment. OCP BBU specifications explicitly reference safety and propagation constraints and relevant certification/testing practices [82], [92]. This strongly motivates designs that (i) enforce conservative SoC windows and thermal monitoring, and (ii) reduce unnecessary cycling.

If the design intent is "UPS-like" ride-through for all computing devices, deployment of BBU on every rack is the straightforward approach used in OCP-style architectures [82], [83], [90]. Selective deployment (e.g., BBUs only on the highest-power or highest-priority racks) can reduce capex and coordination overhead, but it changes the availability model: unprotected racks become dependent on workload-level fault

TABLE III
HIGH-LEVEL COMPARISON OF RACK-LEVEL BBUS AND CENTRALIZED UPS SYSTEMS.

| Aspect | Rack BBUs | Central UPS |
|---|---|---|
| Primary purpose | Rack ride-through; local fault containment [83] | Facility ride-through; centralized management [34] |
| Timescales | Seconds–minutes (backup, recovery) [85] | Minutes+ (backup) and grid services where allowed [86] |
| Sub-second smoothing | Not ideal; accelerates battery aging [87], [72] | Not ideal; GPU transients are localized rail events [72] |
| Coordination burden | High; fleet SoC, recharge scheduling, priority handling [88] | Lower; centralized components |
| Efficiency | Avoids some double conversion [89] | Often involves AC–DC–AC in classic designs |

tolerance, or upstream ESS (BESS/gensets) without transient protection.

### C. Server- and GPU-Level Storage

*1) Capacitors instead of batteries:* The highest-frequency components of AI load power dynamics are at server-level: rapid power consumption swings on the GPUs. These events are handled by local decoupling and bulk capacitance [50]. Buffering at this layer prevents microsecond-to-millisecond disturbances from propagating to the power sharing unit (PSU) and rack bus, reducing upstream stress and allowing higher utilization at the rack power infrastructure [72].

Compared with batteries, supercapacitors tolerate extremely frequent charge–discharge cycles with minimal degradation, making them attractive for sub-second smoothing [93], [94]. Industry offerings and proposals include compact supercapacitor banks intended to suppress short spikes that would otherwise require overbuilding upstream power infrastructure. The main constraint is energy density and physical volume: supercapacitors can buffer transients and short bursts, but they cannot provide minutes of ride-through and therefore complement (not replace) rack BBUs and other upstream ESSs [94].

*2) Firmware/software shaping as energy "storage":* A key trend is co-design of electrical buffering with firmware-level power shaping. Vendors explicitly target smoother power draw by controlling ramp rates and limiting transient excursions. For example, NVIDIA describes firmware-controlled ramp-up behavior and a "power burner" mode to manage ramp-down and stabilize facility-level power dynamics during AI job transitions [14]. At the platform level, software interfaces such as NVIDIA's NVML expose enforced GPU power limits and real-time power telemetry, enabling operators and higher-level controllers to constrain GPU power draw and coordinate device-level consumption with rack- or facility-level power envelopes [95]. It is framed as an industry direction to approach power stabilization as a cross-stack problem that couples hardware energy storage and software control to prevent large excursions and meet grid/facility ramp constraints [50].

### D. Sizing Considerations for Rack- and Server-Level ESSs

Sizing at the rack and server layers is driven by different objectives than grid-scale or UPS-level storage. Rather than energy capacity for extended outages or grid-service participation, the dominant constraints are rack power consumption, backup duration target, and redundancy requirements.

The fundamental BBU shelf sizing requirement is that the shelf must supply the full rack power demand for the target ride-through duration under a single module failure. For AI racks, where power demands can exceed 100 kW and reach MW-scale in dense configurations [80], this places a substantially larger energy requirement on the shelf than in traditional deployments. In ORV3 architectures, the 5+1 redundancy model requires each active module to be sized for its proportional share of the full rack load plus margin [83]. For target backup duration, OCP reference designs reflect a goal of minutes of ride-through [85], [90]. The specific duration that rack-level storage supports should be designed in sync with upstream ESSs, namely BESS or gensets, since its task is to bridge outage onset with extended ESS being online. Extending this window increases energy capacity but consumes already limited rack space, as well as amplifying thermal risks for Li-ion cells colocated with IT equipment [87], [82].

Supercapacitors at the server level are sized to absorb the transient energy of rapid GPU power swings [72]. For sub-second transients, while power swings could be large, the energy required is limited, which makes supercapacitors viable at this layer despite their low energy density [50], [93]. The binding constraint is therefore capacity with regard to the GPU power swing rather than cycle life, since supercapacitors tolerate very high cycle counts with minimal degradation [94], [14].

### E. Coordination Across Rack and Server Layers

Coordination should be explicit about objectives and timescales: GPU/server controllers shape fast dynamics under performance constraints; rack BBU controllers manage SoC availability and recovery without creating recharge spikes at facility level; facility controllers enforce facility envelopes and power-quality limits [88], [96]. OCP rack ecosystems already expose the necessary hooks (telemetry, shelf controllers, parallel shelf operation) to implement multi-layer coordination in practice [82], [83]. Under MVDC architectures, server/GPU capacitive buffering can reduce required BBU power bandwidth and cycling, but does not eliminate the seconds–minutes energy role of BBUs for ride-through and controlled recovery [81].

## VIII. SECOND-LIFE BATTERY ENERGY STORAGE SYSTEMS (SLBESS) IN AI DCS

Having established the functional roles of ESSs across architectural layers, an important practical question concerns cost scalability, motivating the use of second-life batteries (SLBs).

Electric vehicle (EV) batteries are typically retired when they reach around 80% of their initial capacity. Retired batteries can either be sent to recycling facilities or repurposed for secondary applications, giving them a second life. One of the most common second-life applications is stationary BESS for the electric power grid [97]. Many U.S. and Canada based startups have raised funding to re-purpose used batteries. For

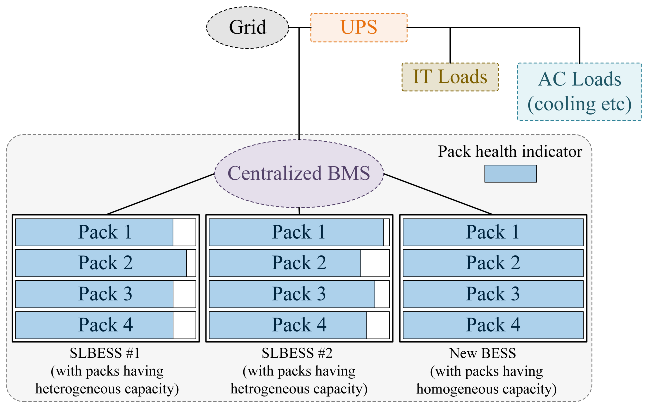


Fig. 6. SLBESS with heterogeneous composition for backup generation of UPS for AI DC load.

example, B2U Storage Solutions [98], Element Energy [99], Moment Energy [100], Smartville [101], and Redwood Energy [102] have each demonstrated the technical and economic viability of SLBs as behind-the-meter (BTM) and front-of-the-meter (FTM) BESS. Beyond technical feasibility and cost savings, the reuse of SLBs confers substantial environmental advantages by decreasing lifecycle emissions and supporting a circular economy [103]. While the application of SLBESS for grid support is well documented, their deployment for AI DC loads is an emerging and promising opportunity, as highlighted in a recent project by Crusoe Energy, where the company installed used batteries to power AI DC load [104]. SLBESS installations must also adhere to battery repurposing standards such as UL 1974 [105]. Therefore, regulatory compliance is mandatory for building AI DC infrastructure and battery reuse.

### A. SLBESS Assisting AI DC On-Site Generation

For AI DC load, SLBESS can serve as BTM generation backup source, provided that the battery packs are rigorously tested and qualified via health metrics. This is a GFL mode of operation where hybrid configurations, combining used and new battery packs, are technically feasible as shown in Fig. 6. The battery management system (BMS) balances the varying capacities of different packs. Additionally, a single SLB pack exhibits heterogeneity across cells and modules, resulting in variable capacities, voltages, and current limits. E.g. a single degraded cell may constrain the performance of an entire module or pack. To solve this, passive and active balancing schemes have been explored to mitigate these challenges. Advanced control architectures have been proposed to actively balance heterogeneous cell capacities in SLBs [106].

### B. Hybrid GiUPS configuration for AI DCs using SLBESS

UPS systems in AI DCs provide instantaneous backup for critical IT loads. This necessitates energy storage solutions capable of sustained discharge durations exceeding 10 hours. SLBESS are generally not suitable for extended durations, and operate within a narrow SoC window to avert deep discharge. This is because the over-discharge accelerates cell-level degradation and may push cells to the non-linear “knee point” region in the degradation curve. Thus, unless carefully derated and managed, SLBESS may offer limited suitability for long-duration UPS applications.

In AI DC, using SLBESS for short-duration backups while avoiding rapid degradation is technically feasible. Optimal dispatch strategies must be implemented to achieve that. Traditionally, the fundamental approach of using BESS involves energy arbitrage, where the BESS charging occurs when electricity prices are low, and discharge occurs when the electricity prices are high. This economic objective is balanced against the physical aging of the battery through a degradation cost component, shown in Eq. 6.

$$\max\,(C_{dis,t}\,P_{dis,t} - C_{ch,t}\,P_{ch,t}) - C_{deg}(\text{cycles}(P_{dis,t}, P_{ch,t})) \tag{6}$$

subject to:

- Battery Constraints that include limits on the SoC and maximum charge/discharge rates to ensure operational safety.
- Grid Constraints that includes power exchange limits and local grid regulations.

For ever time step, $t$ in hours, $C_{dis}$ and $C_{ch}$ are the market price ($/kWh) of electricity during the discharge and charge phase. $P_{dis}$ and $P_{ch}$ are the power output (kW) discharged from and charged to the SLBESS. $C_{deg}$ is the degradation cost coefficient, representing the cost of battery wear per cycle. The cycles of BESS can be calculated as a function of aggregated energy throughput $f(P_{dis},P_{ch})$. The sum of $P_{ch}$ and $P_{dis}$ represents the total power throughput, which serves as a proxy for the stress placed on the SLBESS. To find $C_{deg}$ in $/cycle, the data from an accelerated life testing of SLB cells of corresponding chemistry can be used.

For AI DCs, the primary objective of energy storage optimal dispatch shifts from pure arbitrage to supply guarantee and reliability. In a hybrid GiUPS configuration, the SLBESS must prioritize the load over economic gains. The optimality equation can be modified to include a reliability term, which serves as a significant penalty for unserved load, ensuring the AI DC remains operational. Therefore, Eq. 6 can be modified as Eq. 7

$$\max \begin{pmatrix} C_{\text{dis},t}P_{\text{dis},t} - C_{\text{ch},t}P_{\text{ch},t} \\ -\,C_{\text{deg}}(P_{\text{ch},t} + P_{\text{dis},t}) - C_{\text{reliability}}L_{\text{unserved},t} \end{pmatrix} \tag{7}$$

$C_{reliability}$ is a high-value penalty factor associated with the loss of power to the AI DC (interpreting the ”supply guarantee” requirement from the sources) and $L_{unserved}$ is the portion of the critical AI DC load not met by the grid or the SLBESS while subjected to the BESS and UPS constraints.

On the grid side, GiUPS can be a source of FFR. This is possible with bidirectional rectifiers that can respond to changing grid frequency. FFR tends to use the BESS frequently within a narrow SoC window. SLBESS alone is not suitable for this sort of grid service, leading to its rapid degradation [107]. However, if used alongside a new BESS, the UPS controller can be programmed to leverage the SLBESS for charging the new BESS when its SoC falls below a certain threshold. If optimized, this can reduce the energy import from the grid, saving the cost of energy. Fig.

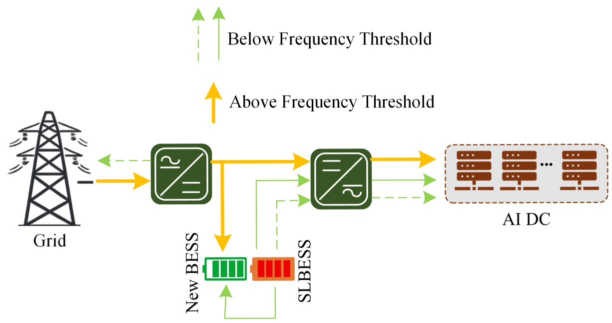


Fig. 7. FFR by utilizing new BESS and SLBESS in GiUPS architecture

7 shows the possible scenarios, which are listed below.

(i) In case of grid frequency above the threshold, the UPS controller charges the new BESS and SLBESS, providing stabilization of the frequency.

(ii) In case of grid frequency below the threshold,
a) The UPS controller can discharge new BESS and provide power back to the grid while powering the IT load with SLBESS.
b)The UPS controller can meet a part of the IT load using the new BESS, and use SLBESS to charge the new BESS and stop any import/export to the grid.

### C. Grid-Scale SLBESS for AI DCs

The US national grid has a long queue for interconnection requests. This leads to limited generation and difficulties in accommodating new AI DC load. In [108], the authors concluded that 76 GW of new load can be integrated without significant upgrades by curtailing 0.25% of new flexible load per year. This amounts to a curtailment of 22 hours/year. FTM grid-scale SLBESS can achieve this by shaving peaks of AI DC load, decreasing the stress on the grid that is caused by erratic peaks of AI DC load. It can also acts as standby generation and partake in resource adequacy. Furthermore, as hyperscalers such as Meta, Microsoft, and Apple Inc. increasingly engage in energy market operations [109], grid-scale FTM SLBESS can be utilized to manage surplus power from renewable generation plants under PPAs enabling these hyperscalers to hedge against increasing energy prices.

By implementing the optimal dispatch strategies previously discussed, these systems can store excess renewable energy during periods of high production or low market cost and sell it back to the wholesale market when prices are high. This strategy is particularly effective when using lithium-ion batteries, such as lithium iron phosphate (LFP), which have been proven to be a viable and high-capacity option for DC loads.

However, to successfully integrate this FTM SLBESS approach into hyperscale infrastructure, several factors must be carefully balanced:

- **Reliability vs. Profit:** While selling energy to the wholesale market provides economic benefits, the dispatch logic must prioritize supply guarantees and the reliability of the AI DC load over arbitrage profits.
- **Degradation Management:** Because these systems utilize second-life battery cells, dispatch strategies must be carefully managed, and aging of the SLBESS must be monitored more rigorously than conventional BESS to prevent accelerated degradation during market participation.
- **System Optimization:** Hyperscalers can leverage real-time SLBESS status to optimize hybrid BESS/UPS system operation, enabling effective peak shaving and grid interaction while maintaining sufficient power reserves for critical AI DC operations.

### D. Cost and Sizing Aspects of SLBESS for AI DCs

*1) Csot:* SLBESS is typically more cost-effective than new BESS. However, cost is influenced by supply, location, and market conditions. The cost of stationary storage declined from \$169/kWh in 2020 to about \$108/kWh in 2025, amounting to 36% reduction worldwide [110]. This decline trajectory may be a hindrance to SLBESS usage in the future. Moreover, refurbishing, operation, and maintenance can constitute a significant portion of CapEx. Market analysis suggests LFP batteries are more economically advantageous for second-life use compared to nickel-rich chemistries, primarily due to the NCX battery's higher recycling value posing a demand competition between SLB repurposers and recyclers [111]. Since reliability can be a huge factor in AI DCs, the hyperscalers may prioritize new BESS over SLBESS. However, the retirement of EV batteries is expected to coincide with rising DC energy demand and the policies, such as the *One, Big, Beautiful Bill Act* (OBBBA) bill, introduce *investment tax credits* (ITC) for battery storage sourced within the country, enhancing the attractiveness of domestically available SLBs for AI DC deployment [112].

*2) Sizing:* Sizing SLBESS for AI DCs presents a distinct engineering challenge. SLBs, repurposed from EV applications, exhibit reduced usable capacity, increased internal resistance, and greater heterogeneity in state-of-health (SoH) compared to new cells [113], [114]. To mitigate accelerated degradation and ensure operational reliability, SLBs are typically operated within narrower SoC windows and under derated conditions [115]. Unlike new batteries that can safely utilize a broad operational SoC range (e.g., 10–90%), second-life systems are often constrained to tighter windows (e.g., 30–70%) to limit stress and extend remaining useful life. This restriction directly reduces the effective usable energy fraction, thereby requiring oversizing in both energy (kWh) and power (kW) capacity relative to the predicted load demand of AI DCs. SLBESS must be sized not only for operational objectives such as FFR, peak shaving, and short-duration backup, but also to satisfy redundancy and fault-tolerance criteria. The SoH variability across SLBs introduces capacity dispersion and imbalance, which must be explicitly accounted for in system-level sizing methodologies [113].

Thermal and cycling considerations further complicate the sizing process. For SLBs with limited remaining useful life (RUL), constraining DoD and per-cycle energy throughput becomes essential to mitigate capacity fade and impedance growth. However, these operational safeguards further reduce usable capacity and necessitate additional oversizing. Moreover, increased internal resistance in aged lithium-ion cells leads to reduced power capability, particularly at lower SoC levels [116]. This reinforces the requirement for power oversizing to ensure that transient load spikes can be supported without violating voltage, thermal, or safety constraints.

## IX. Challenges and Future Directions

### A. Challenges for Integrating ESSs in AI DCs

In the following section the main challenges and gaps are discussed considering multi-level ESSs in AI DCs. As discussed in previous sections, the ESSs not only can support the reliable operation of AI DCs but also can smooth the AI DC grid integration. In addition, it showed that integrating ESSs in different levels in AI DC power infrastructure leads to a grid interactive AI DC that can support the grid in emergency cases like frequency regulation, reactive power compensation or peak shaving scenarios. However, there are still challenges for implementing hierarchical ESSs in AI DCs, which will be discussed in the following sections.

*1) Simulation and Experimental Validation:* To validate the optimal operation of the energy management system (EMS) of an AI DC, it is necessary to model its different components, including the ESSs. To our best knowledge, there is no software specifically developed for simulating EMSs of AI DCs. While MATLAB/Simulink or GT-SUITE software can be used to integrate mechanical and electrical parts in an AI DC, the integration of multiple solvers, electrical units, and mechanical units is not properly supported. Specifically, the multiple power conversion stages inside an AI DC require transient analysis, whereas the thermal units do not have the same requirement [117], [118]. Thus, accurate analysis of ESSs in AI DCs requires a software package that can simultaneously integrate transient and steady-state analyses [29]. On the other hand, the available real-time simulator devices are also not suitable for real-time experimental analysis of AI DCs, since they are primarily developed for analyzing electrical circuits rather than combined systems.

*2) GPU Scheduling:* Current GPU-based AI workloads are predominantly executed at the highest supported core frequency, prioritizing peak performance at the expense of energy efficiency. Unlike CPUs, where dynamic voltage and frequency scaling (DVFS) is a mature and widely adopted mechanism, energy-aware frequency regulation for GPUs remains at an early stage of development [119], [120]. Moreover, existing GPU scheduling policies largely optimize for throughput and latency, without explicitly considering the energy consumption characteristics of heterogeneous deep learning tasks [121], [122]. This limitation is further exacerbated by the fact that many deep learning developers possess limited insight into the underlying hardware behavior of AI workloads. This can accelerate the degradation of ESSs and reveals the lack of control over GPU power profiles, which is essential for power smoothing scenarios.

*3) Distribution Transformers and AI DCs:* Traditional distribution transformers are primarily designed for unidirectional power flow, supplying electricity from the medium-voltage grid to downstream loads, and their deployment in grids with grid-interactive AI DCs introduces new operational challenges. AI DCs equipped with large-scale ESSs and advanced power electronics can dynamically shift between high consumption and active power injection modes for grid services. Under such bidirectional power flow, conventional transformers may experience accelerated thermal aging due to loading patterns and reverse power conditions that deviate from standard design assumptions [60]. Moreover, voltage regulation mechanisms and tap settings optimized for passive load behavior may become ineffective or unstable when facing rapid transitions between load and injection states [123]. These limitations reveal that conventional distribution transformers are not inherently suited for highly dynamic, bidirectional operation driven by GiUPS or BESSs in AI DCs, underscoring the need for enhanced transformer models, real-time monitoring, and power-electronic-aware grid interfaces.

*4) Load Forecasting in AI DCs:* As discussed earlier, the AI DC power profile is hard for forecast. The traditional loads in power grids have predictable trajectories that can be predicted considering the proper historical data. However, this is not applicable for AI DC load profile. As a result, it can directly affected the sizing and ESS operation modes in AI DCs. For instance, the rack-level BESS or chip-level batteries which are designed for power smoothing applications need the accurate power consumption to operate effectively. In addition, the grid-scale BESSs are also need the accurate load profile of the DC to smooth the load and provide effective grid support.

*5) Advanced ESSs Degradation Modeling and Life Time Prediction:* Due to high power variability in AI DCs, more frequent charging and discharging scenarios for ESSs are inevitable. This require a precise degradation analysis to maximize the life time and optimize the ESS operation. As discussed in section VII, the ESS at chip or rack level experiences a very high frequency in different operating conditions to smooth the power profile. In this regard, the online monitoring of the ESS could help for better life time prediction and proactive maintenance operations. As Lithium-ion batteries are more desirable for future AI DCs, the study of cyclic aging is important in both small scale ESSs or large scale BESSs. In addition, the installed SLBESSs in AI DCs are more vulnerable in case of aging and they need more precise monitorization especially for larger scale storage units.

*6) Hierarchical ESSs Coordination:* Multi-level ESS implementation in AI DCs requires a centralized EMS to monitor the operating modes of different ESSs and ensure coordination among them [124]. The on-site grid-scale BESS should operate properly with the GiUPS to enable accurate power sharing, either to efficiently utilize RESs or to support the grid in emergency cases. Moreover, the GiUPS battery size and its switching time are related to the size of the on-site grid-scale BESS. Reliability analysis and cost-comparison analysis are required to determine the optimal combination of both for supplying the AI DC and supporting the power grid. The work [125] demonstrates a novel control framework for utilizing supercapacitors and grid-scale BESS for load smoothing, which shows the potential of hierarchical coordination among ESS units.

TES is also required to operate coherently with the on-site BESS or FC. The BESS absorbs excess power during off-peak periods, and this energy can be utilized to support the TES, as stated in section VI. However, coordinating these systems according to the BESS capacity and its key role in power smoothing or grid support is challenging. In addition, the BBUs and chip-level ESSs should operate together for power smoothing through multi-layer coordination. Thus, ESSs have a direct impact on each other, or at least on their neighboring layers, in a multi-layer structure, which necessitates a centralized control and management system with appropriate data acquisition units.

*7) Long Duration ESSs (LDESSs):* On-site large scale BESSs or GiUPS systems require LDESSs to compensate the intermittency of RESs or providing long lasting AI DC support in case of the utility power failure [126]. The technology for LDESSs is still not mature and further investigation are needed.

*8) Optimal Sizing and Cost Considerations:* There is little public research on the optimal sizing and cost analysis of ESSs inside DCs. In AI DCs, due to the presence of multi-layer ESSs, sizing and cost analysis are even more critical. For instance, is a grid-scale BESS more cost-effective, or a GiUPS system with high power-density batteries? Alternatively, is it more cost-effective to consider large-scale supercapacitors at the rack level, or to use a combination of BBUs and supercapacitors in load-smoothing scenarios? To answer these questions, multiple analyses should be considered to enable precise comparisons.

### *B. Possible Future Directions*

*1) Power-Aware GPU Scheduling:* During the training of deep learning models for predicting responses under different configuration settings, it is essential to jointly learn and optimize both throughput and energy consumption. This requires adaptive strategies for local and global batch size scheduling to balance convergence speed with computational efficiency [127]. Some solutions are discussed in section VII. In addition, GPU resources should be dynamically scheduled across training tasks by accounting for time-varying electricity prices and the availability of renewable energy sources, enabling energy-aware model training [6], [128], [129], [130]. To support such flexibility, elastic resource allocation is a key requirement, allowing the number of GPUs assigned to a training job to be adjusted dynamically during execution without disrupting the learning process. This elasticity enables efficient utilization of heterogeneous compute resources and provides the controllability of GPU power consumption which is necessary for chip-level ESS or BBU scheduling. Beyond this, dynamic batch size selection can be implemented to regulate the utility grid voltage profile [131]. The work [131] demonstrates the potential of chip-level utilization to enhance system-level objectives, in which ESSs implementation can also be included in the optimization problem.

*2) AI DC Load Observability:* High-resolution monitoring of DC load dynamics can be achieved by employing waveform measurement units capable of capturing load profiles at very short time intervals (below 10 ms) [1]. Such fine-grained measurements enable the observation of fast transient behaviors and rapid load fluctuations that are otherwise invisible to conventional metering infrastructure. Building on this high-fidelity data, machine learning techniques can be leveraged to accurately predict short-term and long-term load patterns, supporting proactive control and optimization strategies. Besides, advanced load modeling studies are further increase the load observability of AI DCs not only for short term studies but also for long term planning and operation tasks [132], [133], [134], [135]. Furthermore, close collaboration between utilities and DC operators is essential to enable secure access to real-time load profiles, ensuring data confidentiality while facilitating coordinated grid–DC operation and enhanced system reliability.

*3) Advanced Degradation, State Estimation, and RUL Prediction during operation:* Lithium-ion batteries undergo both calendar degradation and cyclic aging [136]. Calendar degradation is time-dependent and occurs regardless of battery usage, while cyclic degradation results from charge-discharge cycles. Degradation pathways, including solid electrolyte interphase (SEI) growth, lithium plating, and particle fracture [97] lead to capacity fade and increased internal resistance. To avoid the SLBs from entering the non-linear region of the degradation curve, a degradation-aware dispatch strategy needs to be devised. Estimating the RUL of SLBs is essential for safe deployment. Approaches range from data-driven techniques [137], neural network-based models, to entropy-based algorithms [138]. Uniquely, aging curves of SLBs are shaped by first-life usage patterns, making every battery distinct. European Union led Initiative Battery Passport [139] tracks lifecycle data, empowering refurbishers to select candidates for reuse.

*4) FTM grid-scale BESS as A Reliable Reserve:* By monitoring and communicating the grid-scale BESS status, located in AI DC sites, with the grid operator, more optimized reserve planning can be achieved [140], [141]. In this case, the total amount of unused energy of grid-scale BESS can be considered a potential reserve that can be injected into the utility grid during contingency events such as the tripping of synchronous generators. The FTM grid-scale BESS can also play the role of an active reserve source in emergency cases by locally feeding the AI DC load. In this case, the grid operator disconnects the AI DC from the grid and allows the AI DC to supply its load using the available BESS co-generation resources. However, this requires precise coordination and control strategies between both the utility and AI DC owners.

*5) Revisiting SSTs for AI DCs:* SSTs [142], [143], [144] are considered primarily for enabling medium-voltage AC to high-voltage DC conversion (e.g., 800 V DC or higher) to improve rack-level power density in AI DCs [80]. In SST-based architectures, traditional UPS functionalities can be embedded within multi-stage power electronic converters. Moreover, SSTs eliminate the distribution transformer in the AI DC power delivery system, thereby minimizing the side effects of bidirectional power flow. However, SSTs face several challenges including lower reliability due to multi-level, multi-stage power conversion, limited power rating (typically a few MVA) and increased control complexity and cost. While SSTs are attractive for high-density power delivery, they are not yet suitable replacements for UPS systems at gigawatt-scale DCs.

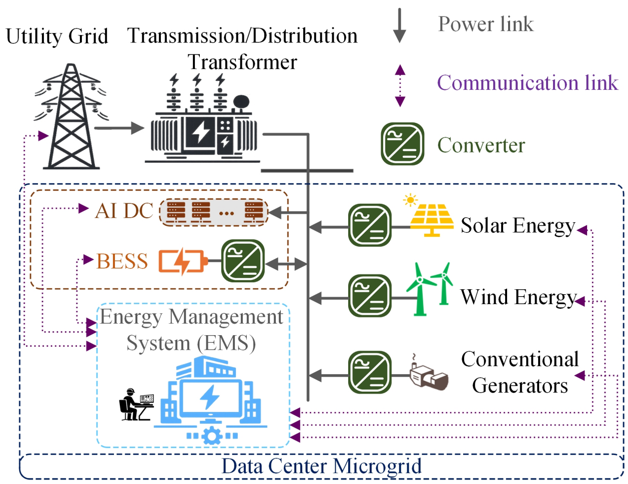


Fig. 8. AI DC microgrid.

Multi-level modular SST architectures, as proposed in recent industry studies, may improve scalability, but reliability and standardization remain key challenges.

*6) AI DC as a Microgrid:* AI DC microgrids adopt hybrid power architectures [145], [146]. These architectures integrate BESS, conventional generators, distributed generation units, and utility grid connections (see Fig. 8). The objective is to achieve high reliability and redundancy. The placement of BESS is a key design choice. Proper placement allows BESS to damp fast load fluctuations. It also improves local voltage and frequency stability. BESS enable coordinated operation among different power generation units. They support grid services such as demand response and peak shaving. They also provide fast reserves. Optimal integration of BESS with other units requires joint power flow and control design. This integration raises the question of BESS versus grid-interactive UPS systems. The boundary between backup and active grid support becomes unclear. In this context, BESS redefine power interface thresholds and reshape power quality metrics. This enables data center microgrids to act as active and flexible grid participants.

## X. Conclusions

This paper provides a comprehensive review of multi-layer ESSs in future AI DCs and their role in supporting both DCs and the utility grid. ESSs ranging from chip-level units to large-scale BESSs are discussed, with particular emphasis on their contribution to grid support and ancillary services. Chip-level ESSs act as the first layer for smoothing heterogeneous GPU power profiles, while large-scale BESSs constitute the final layer in this hierarchical structure. The concept of GiUPS is thoroughly examined, highlighting bidirectional power flow capability as a key enabler of grid-aware UPS design. Moreover, the paper extends beyond battery-based ESSs and investigates the roles of FCs and TEs. FCs are considered a promising alternative to conventional gensets in future AI DCs, offering a lower carbon footprint when using hydrogen. The role of TEs in enabling advanced cooling systems and maximizing the utilization of RESs as on-site generation units is also discussed. SLBESSs offer more cost-efficient solutions for ESS integration but require additional monitorization due to lifetime uncertainties. Furthermore, the main challenges associated with ESS integration in AI DCs are outlined. Finally, as a future direction, the deployment of multi-layer ESS architectures necessitates advanced monitoring systems and EMSs to enable optimal coordination across different layers.

## References

[1] B. Chalamala *et al.*, “Data center growth and grid readiness (tr131),” IEEE Power and Energy Society, Technical Report TR131, 2025.
[2] North American Electric Reliability Corporation (NERC), “Characteristics and risks of emerging large loads,” NERC, White Paper, July 2025, large Loads Task Force (LLTF). [Online]. Available: https://www.nerc.com/globalassets/who-we-are/standing-committees/rstc/whitepaper-characteristics-and-risks-of-emerging-large-loads.pdf
[3] A. Jonker and A. Gomstyn, “What is an ai data center?” 2025. [Online]. Available: https://www.ibm.com/think/topics/ai-data-center
[4] Stream Data Centers, “Data center development in an ai-driven market,” Stream Data Centers, Tech. Rep., Feb. 2024. [Online]. Available: https://www.streamdatacenters.com/wp-content/uploads/2024/02/SDC-BTPS-Whitepaper-240222.pdf
[5] T. McLaughlin, “Big tech’s data center boom poses new risk to us grid operators,” 2025. [Online]. Available: https://www.reuters.com/technology/big-techs-data-center-boom-poses-new-risk-us-grid-operators-2025-03-19/
[6] X. Chen, X. Wang, A. Colacelli, M. Lee, and L. Xie, “Electricity demand and grid impacts of ai data centers: Challenges and prospects,” *arXiv preprint arXiv:2509.07218*, 2025.
[7] E. Ginzburg-Ganz, P. Lifshits, R. Machlev, J. Belikov, Z. Krieger, and Y. Levron, “Technical challenges of ai data center integration into power grids—a survey,” *Energies*, vol. 19, no. 1, p. 137, 2025.
[8] S. Rahman and T. A. Khan, “Energy storage systems for ai data centers: A review of technologies, characteristics, and applicability,” *Energies*, vol. 19, no. 3, p. 634, 2026.
[9] A. Safari, F. Blaabjerg, and A. Oshnoei, “A research-industry perspective of battery systems technology for next-generation data centers,” *Journal of Energy Storage*, vol. 152, p. 120386, 2026. [Online]. Available: https://www.sciencedirect.com/science/article/pii/S2352152X26000502
[10] K. Qian, Y. Xi, J. Cao, J. Gao *et al.*, “Alibaba hpn: A data center network for large language model training,” in *Proceedings of the ACM SIGCOMM 2024 Conference*. New York, NY, USA: Association for Computing Machinery, 2024, pp. 691–706. [Online]. Available: https://dl.acm.org/doi/10.1145/3651890.3672265
[11] N. V. Savant. (2025) Gpu-to-gpu communication: Unlocking parallelism beyond the core. Medium. [Online]. Available: https://medium.com/@nikheelvs/gpu-to-gpu-communication-unlocking-parallelism-beyond-the-core-a80de2974078
[12] North American Electric Reliability Corporation (NERC), “Characteristics and risks of emerging large loads,” North American Electric Reliability Corporation, Tech. Rep., Jul. 2025, large Loads Task Force White Paper.
[13] Atlantic.Net. (2025) An overview of popular nvidia gpus. Atlantic.Net. Accessed: 2026-02-27. [Online]. Available: https://www.atlantic.net/gpu-server-hosting/an-overview-of-popular-nvidia-gpus/
[14] N. S. Rouslan Dimitrov, Harry Petty and M. Blake. (2025) How new gb300 nvl72 features provide steady power for ai. NVIDIA Developer Blog. [Online]. Available: https://developer.nvidia.com/blog/how-new-gb300-nvl72-features-provide-steady-power-for-ai/
[15] Google Cloud. (2024) Accelerating ai inference with google cloud tpus and gpus. Google Cloud Blog. Accessed: 2026-02-27. [Online]. Available: https://cloud.google.com/blog/products/compute/accelerating-ai-inference-with-google-cloud-tpus-and-gpus
[16] Micron Technology. (2024) What changes in storage will ai drive? Micron Blog. [Online]. Available: https://www.micron.com/about/blog/storage/ai/what-changes-in-storage-will-ai-drive
[17] NVIDIA Corporation. (2019) Gpudirect storage: A direct path between storage and gpu memory. NVIDIA Developer Blog. [Online]. Available: https://developer.nvidia.com/blog/gpudirect-storage/
[18] A. Gangidi, R. Miao, S. Zheng, S. J. Bondu, G. Goes, H. Morsy, R. Puri, M. Riftadi, A. J. Shetty, J. Yang, S. Zhang, M. J. Fernandez, S. Gandham, and H. Zeng, “Rdma over ethernet for distributed training at meta scale,” in *Proceedings of the ACM SIGCOMM 2024 Conference*, ser. ACM SIGCOMM ’24. New York, NY, USA: Association for Computing Machinery, 2024, p. 57–70. [Online]. Available: https://doi.org/10.1145/3651890.3672233

[19] NVIDIA Corporation. (2023) Networking for data centers and the era of ai. NVIDIA Developer Blog. [Online]. Available: https://developer.nvidia.com/blog/networking-for-data-centers-and-the-era-of-ai/

[20] S. Sheehan and A. Rakow, "Evolving a data center into a microgrid: Industry perspectives and lessons learned," *IEEE Electrification Magazine*, vol. 11, no. 3, pp. 16–25, 2023.

[21] U.S. Department of Energy. (2025) Advantages and challenges of nuclear-powered data centers. Office of Nuclear Energy. Accessed: 2026-02-27. [Online]. Available: https://www.energy.gov/ne/articles/advantages-and-challenges-nuclear-powered-data-centers

[22] H. Nehrir and C. Wang, "Hydrogen fuel and fuel cells: Potential candidates for sustainable, dispatchable, and environmentally friendly power generation and transport technologies," *IEEE Energy Sustainability Magazine*, vol. 1, no. 3, pp. 52–65, 2025.

[23] Vertiv. (2024) Understanding direct-to-chip cooling in hpc infrastructure: A deep dive into liquid cooling. Vertiv. [Online]. Available: https://www.vertiv.com/en-us/about/news-and-insights/articles/educational-articles/understanding-direct-to-chip-cooling-in-hpc-infrastructure-a-deep-dive-into-liquid-cooling/

[24] M. T. Takci, M. Qadrdan, J. Summers, and J. Gustafsson, "Data centres as a source of flexibility for power systems," *Energy Reports*, vol. 13, pp. 3661–3671, 2025.

[25] A. Karpati, G. Zsigmond, M. Vörös, and M. Lendvay, "Uninterruptible power supplies (ups) for data center," in *2012 IEEE 10th Jubilee International Symposium on Intelligent Systems and Informatics*. IEEE, 2012, pp. 351–355.

[26] A.-H. Fawaz, J. Lorincz, and A. F. Mohammed, "Minimizing data center uninterruptable power supply overload by server power capping," *IEEE Communications Letters*, vol. 23, no. 8, pp. 1342–1346, 2019.

[27] Z. Wang, Z. Yin, J. Yang, and J. Wang, "Coordinated optimization of distributed energy system and storage-enhanced uninterruptible power supply in data center: A three-level optimization framework with model predictive control," *Energy Conversion and Management*, vol. 342, p. 120137, 2025.

[28] J. Paananen, "Grid-interactive data centers enabling energy transition: Data center's hidden potential to provide essential grid services of a future power system," *IEEE Electrification Magazine*, vol. 11, no. 3, pp. 26–34, 2023.

[29] P. Colangelo, A. K. Coskun, J. Megrue, C. Roberts, S. Sengupta, V. Sivaram, E. Tiao, A. Vijaykar, C. Williams, D. C. Wilson *et al.*, "Ai data centres as grid-interactive assets," *Nature Energy*, pp. 1–8, 2025.

[30] A. Di Filippi and L. Valentini, "How to maximize revenues from your data center energy storage system with grid interactive ups," Vertiv, Tech. Rep., 2025, vertiv White Paper.

[31] J. Paananen and E. Nasr, "Grid-interactive data centers: enabling decarbonization and system stability," *Dublin, Ireland*, 2021.

[32] ON.energy, "Hyperscale meets grid stability: On.energy launches medium-voltage ups built for ai data centers," 2025. [Online]. Available: https://www.nacleanenergy.com/alternative-energies/hyperscale-meets-grid-stability-on-energy-launches-medium-voltage-ups-built-for-ai-data-centers

[33] A. Di Filippi and L. Valentini, "How to maximize revenues from your data center energy storage system with grid interactive ups," 2025. [Online]. Available: https://www.vertiv.com/4918e5/globalassets/documents/white-papers/white-paper-maximize-revenues-data-center-energy-storage-grid-ups_329440_2.pdf

[34] Eaton, "Eaton and microsoft's energyaware ups technology pilot project." [Online]. Available: https://www.eaton.com/us/en-us/products/backup-power-ups-surge-it-power-distribution/backup-power-ups/dual-purpose-ups-technology.html

[35] Y. Xie, W. Cui, and A. Wierman, "Enhancing data center low-voltage ride-through," *arXiv preprint arXiv:2510.03867*, 2025.

[36] A. Azizi, S. Morovati, A. Zamani, J. Piruzza, D. Guo, Z. Liu, and P. Taimela, "Strengthening data center operations using grid-forming battery energy storage as a line-interactive uninterruptible power supply," *International Journal of Electrical Power & Energy Systems*, vol. 175, p. 111638, 2026.

[37] C. Tozzi, "Voltage ride-through: A key ingredient in data center resilience," 2026. [Online]. Available: https://www.datacenterknowledge.com/uptime/voltage-ride-through-a-key-ingredient-in-data-center-resilience

[38] J. Conto, Y. Cheng, J. Rose, and J. Schmall, "Texas loads ride toward grid stability: Voltage ride through of large power electronic loads," *IEEE Power and Energy Magazine*, vol. 23, no. 5, pp. 56–67, 2025.

[39] R. Zahedi, A. Zamani, and R. Anilkumar, "Best practices for large load interconnections: A north american perspective on data centers," *arXiv preprint arXiv:2601.12686*, 2026.

[40] R. Li, H. Geng, and G. Yang, "Fault ride-through of renewable energy conversion systems during voltage recovery," *Journal of Modern Power Systems and Clean Energy*, vol. 4, no. 1, pp. 28–39, 2016.

[41] Y. Cheng, M. Sahni, J. Conto, S.-H. Huang, and J. Schmall, "Voltage-profile-based approach for developing collection system aggregated models for wind generation resources for grid voltage ride-through studies," *IET Renewable Power Generation*, vol. 5, no. 5, pp. 332–346, 2011.

[42] D. Pant, A. Singh, G. Van Bogaert, Y. A. Gallego, L. Diels, and K. Vanbroekhoven, "An introduction to the life cycle assessment (lca) of bioelectrochemical systems (bes) for sustainable energy and product generation: relevance and key aspects," *Renewable and Sustainable Energy Reviews*, vol. 15, no. 2, pp. 1305–1313, 2011.

[43] R. Kaiser, "Optimized battery-management system to improve storage lifetime in renewable energy systems," *Journal of Power Sources*, vol. 168, no. 1, pp. 58–65, 2007.

[44] Y. Zhang, Y. Xu, H. Yang, Z. Y. Dong, and R. Zhang, "Optimal whole-life-cycle planning of battery energy storage for multi-functional services in power systems," *IEEE Transactions on Sustainable Energy*, vol. 11, no. 4, pp. 2077–2086, 2019.

[45] J. Wang, S. Ye, B. Wu, and B. Liu, "Life-cycle performance analysis of a building integrated energy system considering equipment performance degradation," *Energy Conversion and Management*, vol. 347, p. 120593, 2026.

[46] M. Kamali and K. Hewage, "Life cycle performance of modular buildings: A critical review," *Renewable and sustainable energy reviews*, vol. 62, pp. 1171–1183, 2016.

[47] N. Omar, M. A. Monem, Y. Firouz, J. Salminen, J. Smekens, O. Hegazy, H. Gaulous, G. Mulder, P. Van den Bossche, T. Coosemans *et al.*, "Lithium iron phosphate based battery–assessment of the aging parameters and development of cycle life model," *Applied Energy*, vol. 113, pp. 1575–1585, 2014.

[48] G. Majeau-Bettez, T. R. Hawkins, and A. H. Strømman, "Life cycle environmental assessment of lithium-ion and nickel metal hydride batteries for plug-in hybrid and battery electric vehicles," *Environmental science & technology*, vol. 45, no. 10, pp. 4548–4554, 2011.

[49] Y. Ding, Z. P. Cano, A. Yu, J. Lu, and Z. Chen, "Automotive li-ion batteries: current status and future perspectives," *Electrochemical Energy Reviews*, vol. 2, no. 1, pp. 1–28, 2019.

[50] E. Choukse, B. Warrier, S. Heath, L. Belmont, A. Zhao, H. A. Khan, B. Harry, M. Kappel, R. J. Hewett, K. Datta *et al.*, "Power stabilization for ai training datacenters," *arXiv preprint arXiv:2508.14318*, 2025.

[51] North American Electric Reliability Corporation (NERC), "Grid forming functional specifications for bps-connected battery energy storage systems," North American Electric Reliability Corporation, White Paper, Sep. 2023. [Online]. Available: https://www.nerc.com/globalassets/our-work/reports/white-papers/white_paper_gfm_functional_specification.pdf

[52] P. Donovan, "Understanding bess: Battery energy storage systems for data centers," Schneider Electric Energy Management Research Center, Tech. Rep. White Paper 185, 2025.

[53] R. H. Lasseter, Z. Chen, and D. Pattabiraman, "Grid-forming inverters: A critical asset for the power grid," *IEEE Journal of Emerging and Selected Topics in Power Electronics*, vol. 8, no. 2, pp. 925–935, 2020.

[54] F. Milano, F. Dörfler, G. Hug, D. J. Hill, and G. Verbič, "Foundations and challenges of low-inertia systems (invited paper)," in *2018 Power Systems Computation Conference (PSCC)*, 2018, pp. 1–25.

[55] F. Blaabjerg, R. Teodorescu, M. Liserre, and A. Timbus, "Overview of control and grid synchronization for distributed power generation systems," *IEEE Transactions on Industrial Electronics*, vol. 53, no. 5, pp. 1398–1409, 2006.

[56] Quanta Tech LLC, "Understanding ai load profiles and their impact on power systems," Online Seminar (Webinar), Sep. 2025.

[57] R. R. Ahrabi, A. Mousavi, E. Mohammadi, R. Wu, and A. K. Chen, "Ai-driven data center energy profile, power quality, sustainable sitting, and energy management: A comprehensive survey," in *2025 IEEE Conference on Technologies for Sustainability (SusTech)*. IEEE, 2025, pp. 1–8.

[58] K. Watson, "Data centers – a good grid citizen," Presentation, Eaton, Jul. 2025, slide on grid support and batteries; Mission Critical Solutions presentation.

[59] X. Tao and R. Gadh, "Coordinated fast frequency response from electric vehicles, data centers, and battery energy storage systems," *arXiv preprint arXiv:2512.14136*, 2025.

[60] I. B. Majeed and N. I. Nwulu, "Impact of reverse power flow on distributed transformers in a solar-photovoltaic-integrated low-voltage network," *Energies*, vol. 15, no. 23, p. 9238, 2022.

[61] L. Pan, M. Song, N. Muzaffar, L. Chen, C. Ji, S. Yao, J. Xu, W. Wu, Y. Li, J. Chen *et al.*, "Salt cavern redox flow battery: The next-generation long-duration, large-scale energy storage system," *Current Opinion in Electrochemistry*, vol. 49, p. 101604, 2025.

[62] A. Mamun, I. Narayanan, D. Wang, A. Sivasubramaniam, and H. Fathy, "Multi-objective optimization of demand response in a datacenter with lithium-ion battery storage," *Journal of Energy Storage*, vol. 7, pp. 258–269, 2016.

[63] G. Ye, J. Fang, N. Wang, Y. Gaogao, and K. Sun, "A grid-forming energy storage system capacity planning method considering device lifetime," *Energies*, 2026.

[64] Y. Yu, K. Shan, H. Tang, and S. Wang, "Reliability and economic impacts of utilizing battery energy storage in data centers for energy flexibility services in smart grids," *Energy Conversion and Management*, vol. 339, p. 119951, 2025.

[65] L. Cupelli, N. Barve, and A. Monti, "Optimal sizing of data center battery energy storage system for provision of frequency containment reserve," in *IECON 2017 - 43rd Annual Conference of the IEEE Industrial Electronics Society*, 2017, pp. 7185–7190.

[66] L. Fan, Z. Tu, and S. H. Chan, "Recent development of hydrogen and fuel cell technologies: A review," *Energy Reports*, vol. 7, pp. 8421–8446, 2021.

[67] D. Manzo, R. Thai, H. T. Le, and G. K. Venayagamoorthy, "Fuel cell technology review: Types, economy, applications, and vehicle-to-grid scheme," *Sustainable Energy Technologies and Assessments*, vol. 75, p. 104229, 2025.

[68] I. Nikiforakis, S. Mamalis, and D. Assanis, "Understanding solid oxide fuel cell hybridization: a critical review," *Applied Energy*, vol. 377, p. 124277, 2025.

[69] I.-B. Kong, W.-S. Kim, and S. Chae, "A grid-forming control method for pemfc power conversion systems with power ramp rate limitation to prevent fuel starvation," *IEEE Open Journal of Power Electronics*, 2025.

[70] F. Perez, "Enabling net zero data centers: A techno-economic analysis of bloom energy's sofc systems," Ph.D. dissertation, Politecnico di Torino, 2025.

[71] K. Nikiforow, J. Pennanen, J. Ihonen, S. Uski, and P. Koski, "Power ramp rate capabilities of a 5 kw proton exchange membrane fuel cell system with discrete ejector control," *Journal of Power Sources*, vol. 381, pp. 30–37, 2018.

[72] Y. Li and Y. Li, "Ai load dynamics–a power electronics perspective," *arXiv preprint arXiv:2502.01647*, 2025.

[73] P. Zheng, X. Xie, C. Zhang, S. Cai, J. Pan, H. Zhang, M. Yan, and Q. Mu, "Techno-economic assessment framework for 2.5 mw-scale grid-connected proton exchange membrane fuel cell power systems: A case study in china," *International Journal of Hydrogen Energy*, vol. 167, p. 150942, 2025.

[74] G. Alva, Y. Lin, and G. Fang, "An overview of thermal energy storage systems," *Energy*, vol. 144, pp. 341–378, 2018.

[75] D. Enescu, G. Chicco, R. Porumb, and G. Seritan, "Thermal energy storage for grid applications: Current status and emerging trends," *Energies*, vol. 13, no. 2, p. 340, 2020.

[76] M. Omrani and M. Ghassemi, "Ai-driven optimization of fan-wall cooling system in a medium-density data center," *International Journal of Heat and Mass Transfer*, vol. 247, p. 127159, 2025.

[77] E. Guelpa and V. Verda, "Thermal energy storage in district heating and cooling systems: A review," *Applied Energy*, vol. 252, p. 113474, 2019.

[78] I. Sarbu and C. Sebarchievici, "A comprehensive review of thermal energy storage," *Sustainability*, vol. 10, no. 1, p. 191, 2018.

[79] C. Luerssen, O. Gandhi, T. Reindl, C. Sekhar, and D. Cheong, "Life cycle cost analysis (lcca) of pv-powered cooling systems with thermal energy and battery storage for off-grid applications," *Applied Energy*, vol. 273, p. 115145, 2020.

[80] J. Huntington and M. Tu, "800 vdc architecture for next-generation ai infrastructure," 2025. [Online]. Available: https://nvdam.nvidia.com/assets/share/asset/zlg5snufeo

[81] IEC, "Medium voltage dc (mvdc) grids for anall-electric society," 2025. [Online]. Available: https://www.iec.ch/basecamp/medium-voltage-dc-mvdc-grids-all-electric-society

[82] D. Sun, D. Shapiro, B. Kim, J. Athavale, and R. Mercado, "Open compute project: Open rack v3 48v bbu (rev 1.4)," 2023. [Online]. Available: https://www.opencompute.org/documents/open-rack-v3-bbu-module-spec-1-4-pdf

[83] D. .Sun, D. Shapiro, B. Kim, J. Athavale, and R. Mercado, "Open compute project: Open rack v3 bbu shelf (rev 1.1)," 2022. [Online]. Available: https://www.opencompute.org/documents/open-rack-v3-bbu-shelf-spec-rev1-1-pdf-1

[84] R. Dimitrov, H. Petty, N. Srivastava, and M. Blake, "How new gb300 nvl72 features provide steady power for ai," 2025. [Online]. Available: https://developer.nvidia.com/blog/how-new-gb300-nvl72-features-provide-steady-power-for-ai

[85] Analog Devices, "Adi ocp orv3 bbu reference design," 2024. [Online]. Available: https://wiki.analog.com/resources/eval/adi-ocp-orv3-bbu-reference-design

[86] Roach, John, "Microsoft datacenter batteries to support growth of renewables on the power grid," 2022. [Online]. Available: https://news.microsoft.com/source/features/sustainability/ireland-wind-farm-datacenter-ups

[87] N. Collath, B. Tepe, S. Englberger, A. Jossen, and H. Hesse, "Aging aware operation of lithium-ion battery energy storage systems: A review," *Journal of Energy Storage*, vol. 55, p. 105634, 2022.

[88] S. Malla, Q. Deng, Z. Ebrahimzadeh, J. Gasperetti, S. Jain, P. Kondety, T. Ortiz, and D. Vieira, "Coordinated priority-aware charging of distributed batteries in oversubscribed data centers," in *2020 53rd Annual IEEE/ACM International Symposium on Microarchitecture (MICRO)*, 2020, pp. 839–851.

[89] A. Safari, H. Sorouri, A. Rahimi, and A. Oshnoei, "A systematic review of energy efficiency metrics for optimizing cloud data center operations and management," *Electronics*, vol. 14, no. 11, p. 2214, 2025.

[90] Bjorlin, Alexis, "Ocp summit 2022: Open hardware for ai infrastructure (grand teton / orv3 rack and power)," 2022. [Online]. Available: https://engineering.fb.com/2022/10/18/open-source/ocp-summit-2022-grand-teton

[91] A. J. Crawford, Q. Huang, M. C. Kintner-Meyer, J.-G. Zhang, D. M. Reed, V. L. Sprenkle, V. V. Viswanathan, and D. Choi, "Lifecycle comparison of selected li-ion battery chemistries under grid and electric vehicle duty cycle combinations," *Journal of Power Sources*, vol. 380, pp. 185–193, 2018.

[92] UL Solutions, "Ul 9540a test method for battery energy storage systems (bess)." [Online]. Available: https://www.ul.com/services/ul-9540a-test-method

[93] D. Genkina, "Will supercapacitors come to ai's rescue? power bursts in large ai workloads can threaten to overwhelm the grid," 2025. [Online]. Available: https://spectrum.ieee.org/supercapacitor-2671883490

[94] Eaton, "Supercapacitors in ai data centers." [Online]. Available: https://www.eaton.com/us/en-us/products/electronic-components/infographics/supercaps-in-ai-datacenters.html

[95] NVIDIA, "Nvml api reference guide - gpu deployment and management documentation," 2025. [Online]. Available: https://docs.nvidia.com/deploy/nvml-api/group__nvmlDeviceQueries.html#group__nvmlDeviceQueries_1gf754f109beca3a4a8c8c1cd650d7d66c

[96] J. Kaur and S. K. Bath, "Harmonic distortion in power systems due to electronic control and renewable energy integration: a comprehensive review," *Discover Electronics*, vol. 2, no. 1, p. 67, 2025.

[97] A. Hassan, S. A. Khan, R. Li, W. Su, X. Zhou, M. Wang, and B. Wang, "Second-life batteries: A review on power grid applications, degradation mechanisms, and power electronics interface architectures," *Batteries*, vol. 9, no. 12, p. 571, 2023.

[98] B2U Storage Solutions, "B2u storage solutions," 2025. [Online]. Available: https://www.b2uco.com/

[99] Element Energy, "Element energy," 2025. [Online]. Available: https://elementenergy.com/

[100] Moment Energy, "Moment energy," 2025. [Online]. Available: https://www.momentenergy.com/

[101] Smartville, "Smartville," 2025. [Online]. Available: https://smartville.io/

[102] Redwood Energy, "Fast, low-cost storage to power the age of ai and a changing grid," 2025. [Online]. Available: https://www.redwoodmaterials.com/news/redwood-energy-fast-low-cost-storage-to-power-the-age-of-ai-and-a-changing-grid/

[103] S. e. a. Bobba, "Life cycle assessment of repurposed electric vehicle batteries: Environmental and climate benefits of second-life use," *Journal of Energy Storage*, vol. 19, pp. 213–225, 2018.

[104] Crusoe Energy and Redwood Materials, "Crusoe and redwood materials power ai/data center infrastructure using second-life ev battery microgrid," Jun. 2025. [Online]. Available: https://www.crusoe.ai/resources/newsroom/crusoe-and-redwood-materials-power-the-future-of-ai

[105] UL, “Ul 1974: Evaluation for repurposing batteries,” 2024. [Online]. Available: https://www.ul.com/services/second-life-electric-vehicle-battery-repurposing-facility-certification

[106] H. Wang, M. Rasheed, R. Hassan, M. Kamel, S. Tong, and R. Zane, “Life-extended active battery control for energy storage using electric vehicle retired batteries,” *IEEE Transactions on Power Electronics*, vol. 38, no. 6, pp. 6801–6805, 2023.

[107] C. White, B. Thompson, and L. G. Swan, “Repurposed electric vehicle battery performance in second-life electricity grid frequency regulation service,” *Journal of Energy Storage*, vol. 28, p. 101278, 2020.

[108] T. H. Norris, T. H. Profeta, D. Patino-Echeverri, and A. Cowie-Haskell, “Rethinking load growth: Assessing the potential for integration of large flexible loads in us power systems,” Nicholas Institute for Energy, Environment & Sustainability, Duke University, Durham, NC, Report, Feb. 2025, report NI R 25-01. [Online]. Available: https://hdl.handle.net/10161/32077

[109] B. Roy. (2025) New power players: How big tech firms are disrupting energy markets. University of Houston Energy. Accessed: 2026-01-24. [Online]. Available: https://www.uh.edu/energy/news/stories/2025/ow_big_tech_firms_are_disrupting_energy_hmarkets.php

[110] BloombergNEF, “Lithium-ion battery pack prices fall to $108 per kilowatt-hour despite rising metal prices,” 2025. [Online]. Available: https://about.bnef.com/insights/clean-transport/lithium-ion-battery-pack-prices-fall-to-108-per-kilowatt-hour-despite-rising-metal-prices-bloombergnef/

[111] A. Bach, S. Onori, S. Reichelstein, and J. Zhuang, “Fair market value of used capacity assets: Forecasts for repurposed electric vehicle batteries,” ZEW – Centre for European Economic Research, Tech. Rep. Discussion Paper No. 25-065, 2025.

[112] Internal Revenue Service (IRS), “Domestic content bonus credit,” 2025. [Online]. Available: https://www.irs.gov/credits-deductions/clean-electricity-production-credit

[113] L. C. Casals, B. A. García, and C. Canal, “Second life batteries lifespan: Rest of useful life and environmental analysis,” *Journal of environmental management*, vol. 232, pp. 354–363, 2019.

[114] E. Martinez-Laserna, I. Gandiaga, E. Sarasketa-Zabala, J. Badeda, D.-I. Stroe, M. Swierczynski, and A. Goikoetxea, “Battery second life: Hype, hope or reality? a critical review of the state of the art,” *Renewable and Sustainable Energy Reviews*, vol. 93, pp. 701–718, 2018.

[115] J. Neubauer and A. Pesaran, “The ability of battery second use strategies to impact plug-in electric vehicle prices and serve utility energy storage applications,” *Journal of Power Sources*, vol. 196, no. 23, pp. 10 351–10 358, 2011.

[116] J. Vetter, P. Novák, M. R. Wagner, C. Veit, K.-C. Möller, J. Besenhard, M. Winter, M. Wohlfahrt-Mehrens, C. Vogler, and A. Hammouche, “Ageing mechanisms in lithium-ion batteries,” *Journal of power sources*, vol. 147, no. 1-2, pp. 269–281, 2005.

[117] Z. Cao, M. Li, F. Lin, J. Jia, Y. Wen, J. Yin, and S. See, “Transforming future data center operations and management via physical ai,” *arXiv preprint arXiv:2504.04982*, 2025.

[118] M. Li, R. Wang, R. Tan, and Y. Wen, “Phythesis: Physics-guided evolutionary scene synthesis for energy-efficient data center design via llms,” *arXiv preprint arXiv:2512.10611*, 2025.

[119] J.-W. Chung, R. Wu, J. J. Ma, and M. Chowdhury, “Where do the joules go? diagnosing inference energy consumption,” *arXiv preprint arXiv:2601.22076*, 2026.

[120] R. Wu, J.-W. Chung, and M. Chowdhury, “Kareus: Joint reduction of dynamic and static energy in large model training,” *arXiv preprint arXiv:2601.17654*, 2026.

[121] J.-W. Chung, Y. Gu, I. Jang, L. Meng, N. Bansal, and M. Chowdhury, “Reducing energy bloat in large model training,” in *Proceedings of the ACM SIGOPS 30th Symposium on Operating Systems Principles*, 2024, pp. 144–159.

[122] J.-W. Chung, J. J. Ma, R. Wu, J. Liu, O. J. Kweon, Y. Xia, Z. Wu, and M. Chowdhury, “The ml. energy benchmark: Toward automated inference energy measurement and optimization,” *arXiv preprint arXiv:2505.06371*, 2025.

[123] R. Frotscher, M. Rave, E. teNyenhuis, and P. Upadhyay, “Reverse power flow impact on transformers,” IEEE PES Transformers Committee Spring 2021 Meeting – Tutorial / Technical Presentation, Apr. 2021, slides. [Online]. Available: https://grouper.ieee.org/groups/transformers/subcommittees/standardsc/C57.133/F24-C57.133-ReversePowerFlowTutorial-%20teNyenhuis.pdf

[124] L. Li, P. Yang, Y. Ju, Z. Hu, and Z. Wang, “Coordinating multiple ups batteries in datacenter for load flexibility and cost reduction,” *SSRN Electronic Journal*, 2025. [Online]. Available: https://ssrn.com/abstract=5647230

[125] M.-S. Ko, J. W. Shim, and H. Zhu, “Mitigation of datacenter demand ramping and fluctuation using hybrid ess and supercapacitor,” *arXiv preprint arXiv:2512.08076*, 2025.

[126] F. Farzan, K. Mahani, F. Farzan, R. Masiello, and W. Brown, “Long-duration energy storage: Planning and operation to enhance power grid sustainability,” *IEEE Energy Sustainability Magazine*, vol. 1, no. 3, pp. 41–51, 2025.

[127] D. Gu, X. Xie, G. Huang, X. Jin, and X. Liu, “Energy-efficient gpu clusters scheduling for deep learning,” *arXiv preprint arXiv:2304.06381*, 2023. [Online]. Available: https://arxiv.org/abs/2304.06381

[128] Y. Wang, Q. Guo, and M. Chen, “Providing load flexibility by reshaping power profiles of large language model workloads,” *Advances in Applied Energy*, p. 100232, 2025.

[129] D. A. Kez and A. Foley, “Instability risks from programmable ai load ramping in low-inertia grids,” *SSRN Electronic Journal*, Jul. 2025. [Online]. Available: https://papers.ssrn.com/sol3/papers.cfm?abstract_id=5370875

[130] C. Crozier and M. Liska, “The potential of data center energy demand to provide grid flexibility,” *Current Sustainable/Renewable Energy Reports*, vol. 12, no. 1, p. 12, 2025.

[131] Z. Liang, J.-W. Chung, M. Chowdhury, J. Chen, and V. Dvorkin, “Gpu-to-grid: Voltage regulation via gpu utilization control,” *arXiv preprint arXiv:2602.05116*, 2026.

[132] S. Lu, C. Xiao, and Y. Weng, “Dynamic load model for data centers with pattern-consistent calibration,” *arXiv preprint arXiv:2602.07859*, 2026.

[133] M. Mughees, Y. Li, Y. Chen, and Y. R. Li, “Short-term load forecasting for ai-data center,” in *2025 IEEE Power & Energy Society General Meeting (PESGM)*. IEEE, 2025, pp. 1–5.

[134] H. Jiang, B. Qu, J. Zhu, F. Zeng, X. Lin, and W. Zhong, “Hyperload: A cross-modality enhanced large language model-based framework for green data center cooling load prediction,” *arXiv preprint arXiv:2512.19114*, 2025.

[135] R. Mo, W. Lin, G. Liu, H. Liu, and L. He, “Learning from imbalance: Cross-server power prediction in large data centers via domain adaptation regression,” *Expert Systems with Applications*, vol. 287, p. 127845, 2025.

[136] G. P. Kostenko, “Accounting calendar and cyclic ageing factors in diagnostic and prognostic models of second-life ev batteries,” 2024.

[137] X. Cui, M. A. Khan, S. Singh, R. Sharma, and S. Onori, “Toward a bms 2.0 design framework: Adaptive data-driven state-of-health estimation for second-life batteries with bibo stability guarantees,” *IEEE Transactions on Transportation Electrification*, 2025.

[138] B. Strugnell-Lees, E. Evdokimova, and T. Wik, “An entropy-based, self-adaptive predictive algorithm for battery degradation,” 2024.

[139] European Union, “Regulation (eu) 2023/1542,” 2023. [Online]. Available: https://eur-lex.europa.eu/eli/reg/2023/1542/oj

[140] B. Xu, Y. Wang, Y. Dvorkin, R. Fernández-Blanco, C. A. Silva-Monroy, J.-P. Watson, and D. S. Kirschen, “Scalable planning for energy storage in energy and reserve markets,” *IEEE Transactions on Power Systems*, vol. 32, no. 6, pp. 4515–4527, 2017.

[141] N. Padmanabhan, M. Ahmed, and K. Bhattacharya, “Battery energy storage systems in energy and reserve markets,” *IEEE Transactions on Power Systems*, vol. 35, no. 1, pp. 215–226, 2020.

[142] D. Rothmund, T. Guillod, D. Bortis, and J. W. Kolar, “99% efficient 10 kv sic-based 7 kv/400 v dc transformer for future data centers,” *IEEE Journal of Emerging and Selected Topics in Power Electronics*, vol. 7, no. 2, pp. 753–767, 2019.

[143] A. Sidorov, G. Zinoviev, and J. Petzoldt, “Solid state transformer as a part electrical circuit for data center application,” in *2021 IEEE 22nd International Conference of Young Professionals in Electron Devices and Materials (EDM)*. IEEE, 2021, pp. 354–359.

[144] A. Q. Huang, “Medium-voltage solid-state transformer: Technology for a smarter and resilient grid,” *IEEE Industrial Electronics Magazine*, vol. 10, no. 3, pp. 29–42, 2016.

[145] J. Irion, P. Wiesner, J. Bader, and O. Kao, “Optimizing microgrid composition for sustainable data centers,” in *Proceedings of the SC’25 Workshops of the International Conference for High Performance Computing, Networking, Storage and Analysis*, 2025, pp. 1990–1996.

[146] Y. Zhang, H. Tang, H. Li, and S. Wang, “Unlocking the flexibilities of data centers for smart grid services: Optimal dispatch and design of energy storage systems under progressive loading,” *Energy*, vol. 316, p. 134511, 2025.